In This Issue:

Articles

Technical News Briefs

Conference Reports

Journal of Research of the National Bureau of Standards

High Precision Microcalorimetry: Apparatus, Procedures, and Biochemical Applications

Volume 91 Number 3 May–June 1986

D. K. Steckler, R. N. Goldberg, Y. B. Tewari, and T. J. Buckley

National Bureau of Standards
Boulder, CO 80303

Apparatus and procedures used for high-precision microcalorimetric measurements are described. The calorimeter is of the heat-conduction type and utilizes semi-conductor thermoelectric modules. The bicompartmental reaction vessel is made of high-density polyethylene and holds about 0.5 mL of solution in each compartment. Imprecision of heat measurement is 0.2 percent when measuring 300 mJ of heat produced by a rapid chemical reaction. Three microcalorimeters are operated simultaneously using a microcomputer and a data acquisition system. Thermochemical and kinetic applications are described. The acquisition of data from an isoperibol solution calorimeter is also described.

Key words: biochemistry; chemical thermodynamics; enthalpy; enzyme-catalyzed reactions; heat-conduction microcalorimetry; isoperibol solution calorimetry; kinetics.

Accepted: February 25, 1986

1. Introduction

Microcalorimetry is an important technique for the measurement of heats of reaction in solution. Since small amounts of solution (typically less than one mL) are required, the technique finds many applications in the study of biochemical and biological systems [1,2][1]. It is the purpose of this paper to describe the microcalorimetric procedures and techniques currently used in the Chemical Thermodynamics Division at the National Bureau of Standards, with particular emphasis on the digital data acquisition system used for the collection and treatment of the experimental data. The simultaneous operation of three microcalorimeters as well as the treatment of experimental data is accomplished with this system. These microcalorimeters have been used in an extensive series of studies of the thermodynamics of enzyme-catalyzed reactions. The calorimeters and the associated data acquisition system can also be used to study the kinetics of enzyme-catalyzed reactions including the measurement of enzyme activity.

Recently, a multi-chambered microcalorimeter has been described by Prosen, Brown, Frohnsdorff, and Davis [3]. Since it contains four microcalorimeters in a single block, it has the advantage that one of the microcalorimeters can be used as a thermal reference or "tare" while the other three are used to monitor processes of interest. This arrangement allows one to carry out long-term studies, e.g., cement hydration. For reactions which are complete within a few hours, the use of a single microcalorimeter has proved successful.

The interfacing techniques used for the microcalorimeters are similar to those needed for the operation of an isoperibol solution calorimeter. This type of calorimeter is useful, in conjunction microcalorimeters described herein, for the study

About the Authors: All are with the Chemical Thermodynamics Division in NBS' Center for Chemical Physics.

[1] Figures in brackets indicate literature references.

of processes in aqueous solution. The computer software used for the acquisition and treatment of experimental data from both the microcalorimeters and the solution calorimeter is described in a separate publication [4].

2. Apparatus

Our microcalorimeters are modelled after the one described by Prosen [5], a schematic of which is shown in figure 1. Essentially, it is a heat-conduction microcalorimeter[2] which accommodates a single bicompartmental reaction vessel. The thermopile assembly consists of a pair of bismuth selenide–bismuth telluride–bismuth antimonide thermoelectric modules (Cambion Corporation, model No. 3958-1)[3] electrically connected in series so that the resultant thermopile voltage is the sum of the voltages of the individual thermoelectric modules. Between the thermoelectric modules, D, is sandwiched a rectangular copper container, E, (3.10 cm wide by 3.10 cm high by 1.27 cm thick) which accommodates the reaction vessel. The thermoelectric modules and the copper container are held in place by means of adhesive. This assembly sits in the middle of a bevelled aluminum block, C, (17.8 cm long, 15.2 cm wide) which is supported by hollow nylon rods, G, (1.27 cm diameter, 0.32 cm wall thickness) within an inner aluminum cylinder, B, (25.1 cm diameter by 20.3 cm long with wall thickness of 1.27 cm and 1.27 cm thick end plates) that is thermostatted to within 0.2 mK per day. This inner aluminum cylinder resides within an outer aluminum cylinder, A, (32.1 cm diameter by 40.6 cm long with wall thickness of 0.95 cm and 1.27 cm thick endplates) and is separated from it by $\approx$2.5 cm of polyurethane insulation, H. The copper leads to the calibrating heater and to the thermopiles are carefully thermally tempered to the aluminum block and pass through holes drilled through that block before leaving the calorimeter via the hollow nylon rods, G.

The bicompartmental calorimetric reaction vessels (see fig. 2) are made of high-density polyethylene (0.762 cm thick by 2.54 cm high with 0.050 cm walls). The two compartments are not equal in size; one side holds 0.55 mL of solution

[2] In a heat-conduction calorimeter the reaction vessels is in good thermal contact with a thermopile which, in turn, is in good thermal contact with the heat-sink or block. Thus, most of the heat generated in the reaction vessel flows through the thermopiles to the block. The voltage generated by the thermopile is a measure of the power produced in the reaction vessel [6].

[3] Certain commercial materials and apparatus are identified in this paper to specify adequately the experimental procedures. Such identification does not imply recommendation or endorsement by the National Bureau of Standards.

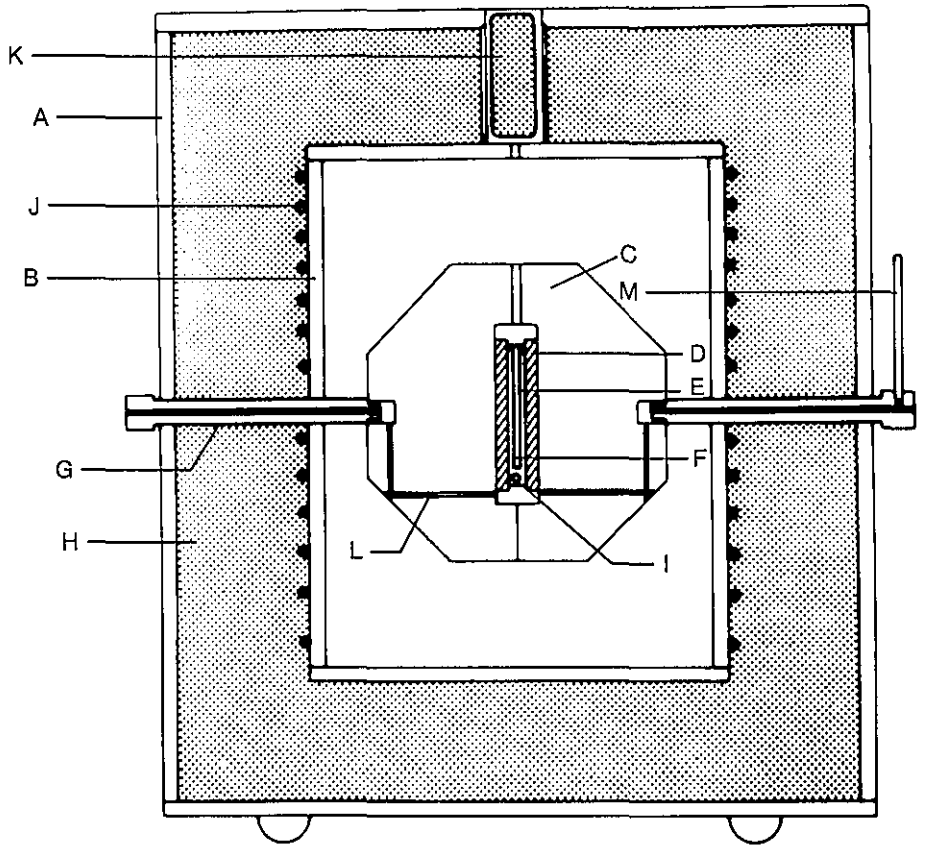

A - Outer Aluminum Cylinder
B - Inner Aluminum Cylinder
C - Aluminum Block
D - Thermoelectric Module
E - Copper Container
F - Reaction Vessel
G - Nylon Rod
H - Polyurethane Insulation
I - Calibration Heater
J - Wires Wrapped on Inner Aluminum Cylinder
K - Entrance Port for Reaction Vessel
L - Hole in Aluminum Block for Wires
M - Handle for Rotation of Block

Figure 1–Schematic cross-section of microcalorimeter (c. f. [5]).

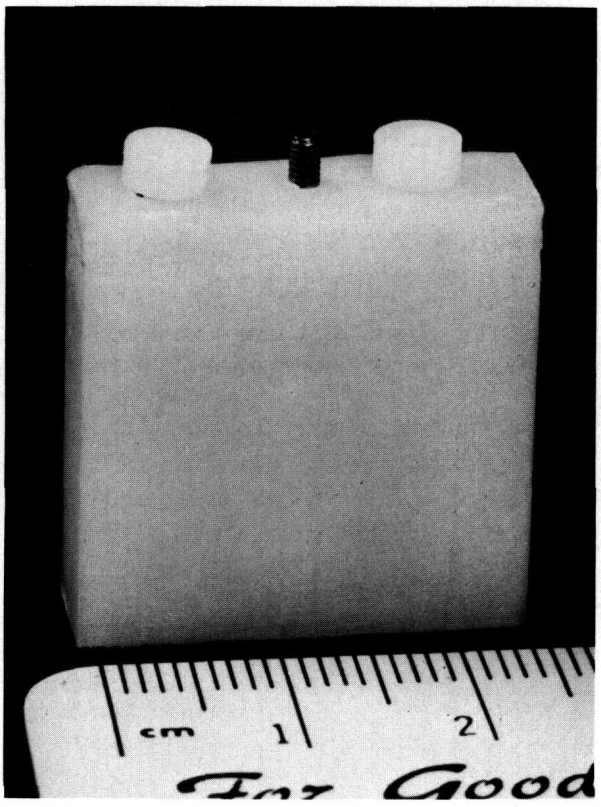

Figure 2–Photograph of high-density polyethylene reaction vessel with O-rings and Teflon plugs in place.

and the other side holds 0.45 mL. Seals are made by compressing Teflon plugs thru the two No. 5-187 Buna-n O-rings which are seated in the filling holes of the reaction vessel. Each reaction vessel is provided with a male stud for connection to a threaded bakelite rod which is used for installation and removal of the cell within the calorimeter. Mixing of the solutions within the reaction vessel is accomplished by rotation of the aluminum block using a handle attached to the nylon support rods. During rotation, the reaction vessel is held in place in the rectangular copper container by means of a piece of phosphor-bronze sheet metal (0.025 cm thick) which is permanently attached to the inside of the rectangular copper container.

The temperature of the inner aluminum cylinder is controlled by means of a Wheatstone bridge circuit. Two arms of the bridge (No. 40 AWG formvar insulated manganin wire) are wrapped around the inner aluminum cylinder; the third arm (No. 40 AWG "99 alloy" formvar insulated wire) is also wrapped around this cylinder; and the fourth arm is a variable resistance box which is kept external to the calorimeter. This resistance box is used to set the temperature of an individual calorimeter. The voltage source for the Wheatstone bridge is a 1.5 V "Batt-sub." The bridge imbalance is amplified by an operational amplifier contained in a current-adjusting type controller (Leeds and Northrup Electromax V). The controller uses both proportional and reset model of operation which are adjusted to obtain a rapid control response with a minimum of overshoot or cycling. The current output from the controller is amplified using a dc power supply and a field-effect transistor amplifier network, and then passed through No. 30 AWG formvar insulated manganin wire which is wrapped around the inner aluminum cylinder. The manganin and the "99 alloy" wires are kept electrically insulated ($>10^8$ ohms) from each other and from the aluminum cylinder by wrapping the aluminum cylinder with a Kimwipe and then coating it with insulating varnish. A second Kimwipe is similarly attached and covers all of the wires that are wrapped around the inner cylinder. All wires are bifilarly wrapped.

A calibrating resistance heater (No. 42 AWG formvar insulated manganin, ≈ 160 ohms) is bifilarly wrapped around a piece of copper wire (No. 20 AWG heavy formvar insulated) which is then placed into a hole in the bottom of the copper container. The heater leads (No. 34 AWG enamelled copper wire) are soldered to the heater and thermally tempered to the copper container for a length of 8 cm. A similar amount of thermal tempering is also done to the copper heater leads at the aluminum block. Potential leads are attached to the copper wire at the point at which they first make contact with the aluminum block after coming from the copper container. Thus, a small heater lead correction (0.013%) is applied during electrical calibration of a calorimeter [7].

Electrical calibration of the calorimeter is performed by measuring (Hewlett Packard 3450A digital voltmeter, inaccuracy less than 0.002%) the voltage across the calibration heater located in the copper container and that across a 1000 ohm standard resistor connected in series with it. Current is supplied from a constant-current dc power supply (Sorensen QHS 40–.5, instability less than 0.001% over a one hour period). Time interval measurement is done using a digital counter (Hewlett Packard 5325B) having a resolution better than one millisecond. The calibration constant of a calorimeter, expressed in W V^{-1}, is measured [6] 1) as the ratio of the steady-state electrical power delivered via the calibrating heater to the steady-state voltage developed by the thermopile during calibration and 2) as the ratio of the total heat deliverd via the calibrating heater to the total area under the voltage-versus-time curve associated with the electrical heat input.

The thermopile voltage from each calorimeter is amplified using a nanovolt amplifier (Keithley model 140, gain linearity 5 ppm, gain accuracy 100 ppm, noise <30 nV peak-to-peak). The gain accuracy was verified using a voltage divider consisting of NBS calibrated 1Ω and 10 kΩ standard resistors in series. A potential difference of 10 V is maintained across these two resistors and the voltage across the 1 Ω standard resistor is amplified at a nominal gain of 10,000 using a nanovolt amplifier. Measurement of the voltage across the two standard resistors and of the amplifier output together with the values of the resistors yields the gain of the amplifier.

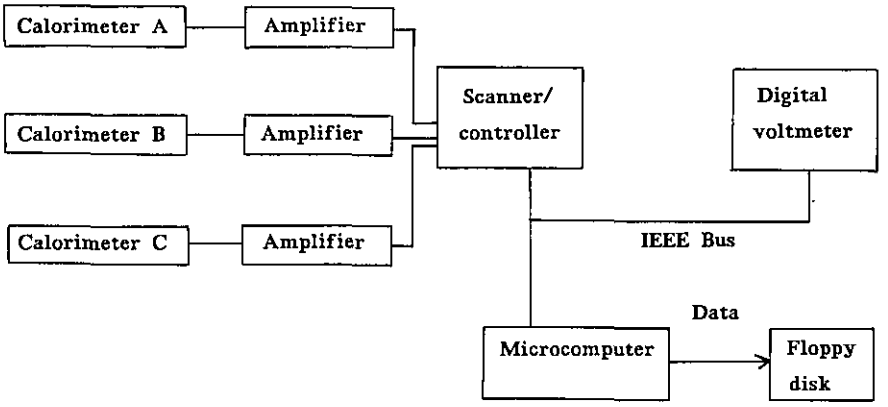

Figure 3–Schematic of data acquisition system for microcalorimeters.

The data collection system is shown schematically in figure 3. The microcomputer is an Apple IIe with two floppy disk drives, a dot matrix printer, a color video monitor, and several cards. The cards in the microcomputer are: 1) clock, parallel and serial interfaces, 2) IEEE-488 communications bus controller, 3) 128 kbyte RAM, 4) 80 column display, and (5) Z–80 microprocessor. All data recording electronics are IEEE-488 bus instruments. They are a digital voltmeter (Hewlett Packard 3456A, inaccuracy <0.002%) and a scanner/data acquisition/control unit (Hewlett Packard 3457A). In-house software was written to control the experiments and to analyze the data.

The temperatures of the microcalorimeters are measured using either a platinum resistance thermometer and a resistance bridge (0.00001 Ω sensitivity) or with mercury-in-glass thermometers having a readability of about 0.02 K. In either case, the thermometer is placed directly into the rectangular copper container in which a reaction vessel is normally placed.

In principle, the calorimeters can operate up to the temperature at which the thermopile units will fail (≈120 °C). A problem which arises at higher temperatures (≈60 to 70 °C) is that the high-density polyethylene reaction vessels expand and thus, if a vessel is introduced into a calorimeter at a lower temperature, that vessel will be extremely difficult to remove after it has reached the temperature of the calorimeter. This problem can be remedied by reducing the thickness of the reaction vessels.

The isoperibol solution calorimeter has been previously described [8]. The principal modification to it is that a digital counter (Hewlett Packard 5334A) is now used to measure the frequency of the quartz-crystal oscillator used for temperature measurement in the calorimeter vessel. The counter is interfaced via the data acquisition/control unit and the IEEE bus to the microcomputer. A schematic of the data acquisition system used for the solution calorimeter is shown in figure 4.

All measuring apparatus were calibrated using standards traceable to NBS. Specifically, the standard resistors and standard cells used in our instrument rack were calibrated by the Electricity Division at NBS, the counter used for time interval

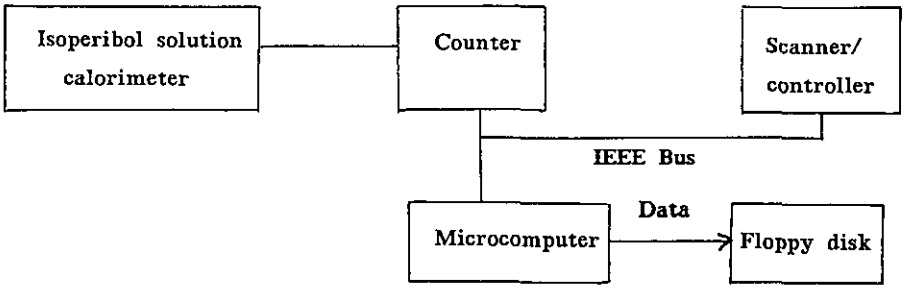

Figure 4–Schematic of data acquisition system for isoperibol solution calorimeters.

measurement was calibrated using the NBS 10 kHz standard frequency, and a capsule-type platinum resistance thermometer was calibrated by the Temperature and Pressure Division at NBS. The resistance bridge used for temperature measurement and the digital voltmeters were calibrated using, respectively, the calibrated resistors and standard cells. The balance used for mass determinations was calibrated using an NBS calibrated set of class M weights.

3. Procedures

The cleaning and loading of the bicompartmental reaction vessels has been found to be an important aspect in achieving good reproducibility. Thus, an ultrasonic cleaner is used for cleaning the reaction vessels following the initial removal and/or inactivation of the solutions in the vessel; for example, a saturated aqueous solution of urea is added to a vessel which contained an active enzyme in solution. Following ultrasonic cleaning, the vessels are rinsed 10 times with distilled water, air dried for several minutes, and then stored in a vacuum desiccator over a drying agent.

The loading of the reaction vessels with solutions is done using a Teflon tipped syringe to avoid problems with droplets which can adhere to metal needles. Avoiding the use of metal objects also helps to mini-mize the chance of damage to the O-ring seats on the reaction vessels. Since the amounts of solution are determined gravimetrically, the vessels are allowed to stand in the balance case in which the weighings are done to minimize both thermal and electrostatic effects. A bottle containing a uranium salt is also kept in the balance case to aid in dissipating any charges. Following loading of a vessel, it is placed into an aluminum block thermostatted at a temperature close to that of the aluminum block in the calorimeter. This pre-equilibration helps to minimize the thermal shock to the calorimeter block. Finally, the reaction vessels are loaded into the calorimeters via the entrance ports and allowed to equilibrate for about one hour. Following equilibration, the calorimeter blocks are rotated several times to mix the contents of the reaction vessels.

The acquisition of data can be broken down into three periods: a fore-period during which the block and reaction vessel are in thermal equilibrium and during which no process heat is produced; a reaction or main-period during which process heat is liberated and flows thru the thermopiles to the block; and an after-period during which no process heat is produced and by which time the reaction vessel and block are again in thermal equilibrium. Recording of the data is typically commenced a few minutes prior to the initiation of the reaction being studied and is continued at 5-second intervals until the conclusion of the after-period. A typical microcalorimetric thermogram is shown in figure 5. During an experiment the amplified voltage data from each microcalorimeter is displayed in a different color on the video monitor. At the conclusion of an experiment, the voltages are recorded on a floppy disk and then analyzed using appropriate computer codes [4].

4. Performance Characteristics

The performance characteristics of the instrumentation are summarized in table 1. Note that the principal limitation on the measurement of small quantities of heat is the magnitude and reproducibility of the "blank" heat of mixing, i. e., the heat effect associated with the mixing of a solution with itself. This effect is dependent upon the solutions being mixed and thus should be determined for each separate investigation in appropriate control experiments.

In table 1 the quantity F is the calibration constant of a calorimeter. Thus, the measured power (dq/dt) is given by

$$dq/dt = F \cdot E \tag{1}$$

where E is the measured voltage relative to a baseline voltage. The total heat measured is given by integration of the area under the curve in a microcalorimetric thermogram [7].

The variation of the calibration constant with temperature can be described by the equation:

$$F = A + B\,T + C\,T^2 \tag{2}$$

where T is the temperature in Celsius. Typical values of the temperature coefficient parameters are: A, 19 to 23 $W\,V^{-1}$; B, -0.07 to -0.08 $W\,V^{-1}\,K^{-1}$; and C, 0.0004 to 0.0005 $W\,V^{-1}\,K^{-2}$.

5. Thermochemical Applications

These microcalorimeters have been used in a series of investigations of the thermodynamics of enzyme-catalyzed reactions (see table 2 and the references contained therein). In addition to their inherent biochemical importance, several of these studies involved reactions of either current or potential industrial importance such as the manufacture of fructose, which is the principal constituent

of corn syrup, and aspartate which is used in the sweetener "Aspartame."

In most of these studies, equilibrium constants have been determined as a function of temperature using chromatographic techniques. Thus, chromatography has been used to measure the extents of the reactions and to detect the presence of any side reactions. Direct heat measurements provide an accurate and direct determination of the enthalpy change for a process. Thus, the combination of equilibrium constants, determined via chromatography or other methods, and enthalpy changes determined from calorimetric measurements are needed to establish and improve the accuracy of the final set of thermodynamic parameters (ΔG, ΔH, ΔS and ΔC_p) for a given process. A knowledge of these thermodynamic parameters allows one to accurately model the behavior of the chemical process of interest over a wide range of temperatures. The combined measurement techniques, microcalorimetry, and chromatography, thus complement each other and are a valuable combination in studying biochemical processes.

6. Application to Measurement of Enzyme Activity and Kinetics

The discussion that follows assumes that the enzyme-catalyzed reaction being studied follows Michaelis-Menten kinetics. The assumed mechanism is:

$$E+S=E\cdot S=E+P \tag{3}$$

where the enzyme, substrate, and products in aqueous solution are designated as E, S, and P, respectively. E·S is the enzyme-substrate complex and the k_i are rate constants. There are three processes to be considered:

$$E+S=E\cdot S \tag{4}$$

$$E\cdot S=E+P \tag{5}$$

and

$$S=P\,. \tag{6}$$

Process (6) is the sum of processes (4) and (5). If at the start of a reaction the enzyme concentration is

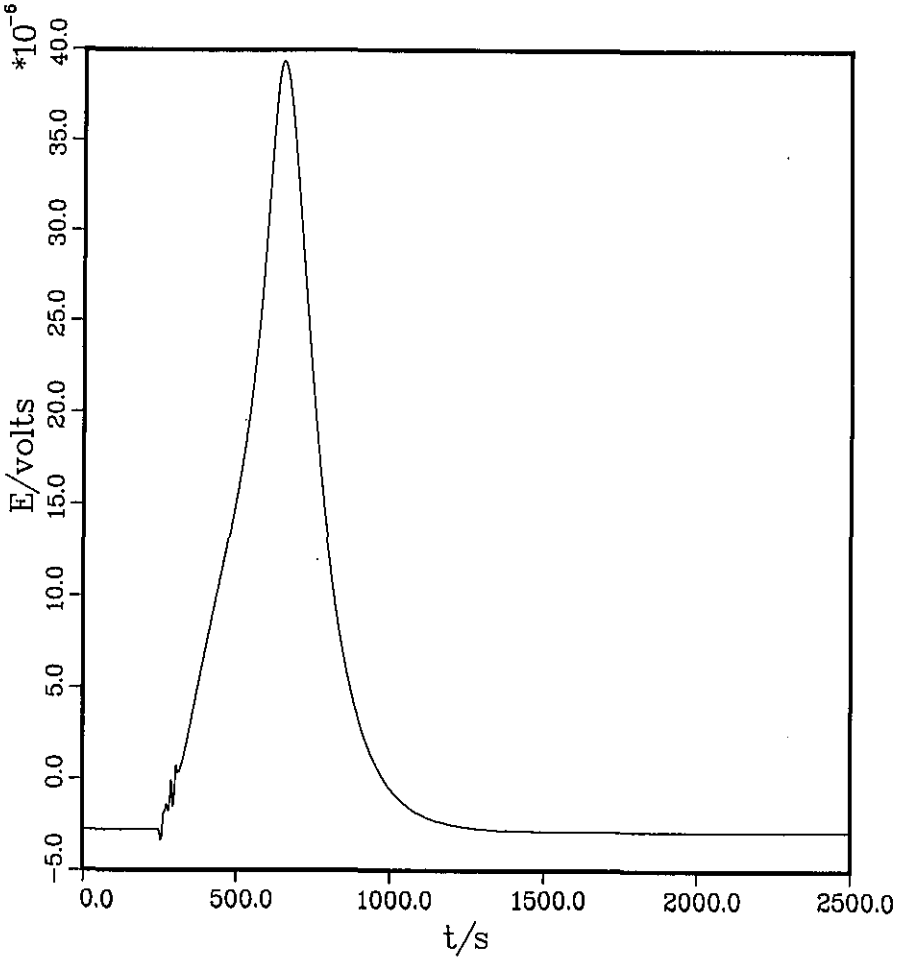

Figure 5–Microcalorimetric thermogram of an enzyme-catalyzed reaction: the hydrolysis of adenosine 5′-triphosphate (ATP) to adenosine 5′-diphosphate (ADP) and inorganic phosphate using *meromyosin*. The irregularities at the beginning of the main or reaction period are attributable to mixing effects. The measured heat effect is 238.0 mJ.

Table 1. Performance characteristics of microcalorimetric instrumentation at 25 °C.

Characteristic	
calibration constant (F)	16 to 22 W V^{-1}
sensitivity (1/F)	0.045 to 0.059 V W^{-1}
noise level of baseline	20 nV peak-to-peak
detectability (1/3 × noise level/sensitivity)	0.15 μW
stability of baseline	100 nV over 24 hours
linearity of calibration constant	0.1 percent from 0.01 mW to 2 mW
time constant[a]	63 s
stability of calibration constant	0.2 percent over 2 years
imprecision[b]:	
q ≈ 10 mJ	0.3%
q ≈ 100 mJ	0.1%
q ≈ 500 mJ	0.05%
q ≈ 300 mJ (chemical heat)	0.2%
"blank" heat effects:	
no reaction vessel in place	0.023±0.03 mJ
empty vessel in calorimeter	−0.065±0.06 mJ
H_2O	0.67±0.22 mJ
human serum	−0.75±1.0 mJ
glucose isomerase (T=25 °C)	−101±4 mJ
inaccuracy[c]	<0.2%

[a] A reaction vessel containing 1.0 mL of water was in the copper container.
[b] Based upon experiments in which electrical heat was introduced for periods of 10 to 100 seconds. All uncertainties are standard deviations.
[c] The inaccuracy was assessed by the performance of both heater placement tests [1] and by measurements of heats of neutralization of HCl with excess NaOH.

e_0 mol L^{-1} and the substrate concentration is s_0 mol L^{-1}, at time t the concentrations are given in terms of the extent of reaction variables (ξ) for the above processes:

$$[E] = e_0 - \xi_4 + \xi_5 \quad (7)$$
$$[S] = s_0 - \xi_4 \quad (8)$$
$$[E{\cdot}S] = \xi_4 - \xi_5 \quad (9)$$
$$[P] = \xi_5 . \quad (10)$$

The rate equations are:

$$d[E{\cdot}S]/dt = k_1[E][S] - k_{-1}[E{\cdot}S] - k_2[E{\cdot}S] + k_{-2}[E][P] \quad (11)$$
$$d[S]/dt = -k_1[E][S] + k_{-1}[E{\cdot}S] \quad (12)$$
$$d[P]/dt = k_2[E{\cdot}S] - k_{-2}[E][P] . \quad (13)$$

At any given time, the instantaneous rate of heat production (dq/dt) is given by:

Table 2. Reactions in aqueous solution which have been studied in our microcalorimeters.

Process	Enzyme	Reference
glucose + ATP^{4-} = glucose 6-phosphate^{2-} + ADP^{3-} + H^+	*hexokinase*	[9,10]
mannose + ATP^{4-} = mannose 6-phosphate^{2-} + ADP^{3-} + H^+	*hexokinase*	[9]
fructose + ATP^{4-} = fructose 6-phosphate^{2-} + ADP^{3-} + H^+	*hexokinase*	[9]
glucose = fructose	*glucose isomerase*	[11]
xylose = xylulose	*glucose isomerase*	[12]
ribose = ribulose = arabinose	*glucose isomerase*	[13]
fumarate^{2-} = malate^{2-}	*fumarase*	[14]
aspartate$^-$ = fumarate^{2-} + NH_4^+	*aspartase*	[15]
$ATP^{4-} + H_2O$ = $ADP^{3-} + HPO_4^{2-} + H^+$	*meromyosin*	[16]

$$dq/dt = k_1[E][S](\Delta H_A) + k_{-1}[E{\cdot}S](-\Delta H_A) + k_2[E{\cdot}S](\Delta H_B) + k_{-2}[E][P](-\Delta H_B) . \quad (14)$$

In general the rate of heat production is a function of four individual rate constants and of two enthalpies in addition to the initial concentrations of enzyme and substrate. Since the time constants of the microcalorimeters are 63 s, the power (dq/dt) must be obtained by deconvolution of the experimental thermogram. If however, slow processes are being studied the deconvolution corrections become negligible. A simplification can be obtained by consideration of the two limiting cases that are now discussed. If the concentration of substrate is much larger than that of the enzyme, the rate of formation of product is proportional to the concentration of the (active) enzyme:

$$d[P]/dt = \lambda_1[E] \quad (15)$$

where λ_1 is an empirical rate constant. If a microcalorimetric experiment is performed where a small amount of enzyme is mixed with a large excess of substrate, the power evolved is:

$$dq/dt = (d[P]/dt)(dq/d[P]) = -[E]\, V \Delta H_6 \quad (16)$$

where V is the volume of solution present and ΔH_6 is the molar enthalpy difference between P and S. The enzyme activity is a measure of the number of moles of substrate converted to product in a given period of time. It is given by:

$$\begin{aligned} dn/dt &= (dq/dt)/(dq/dn) \\ &= -(dq/dt)/\Delta H_6 . \end{aligned} \tag{17}$$

Thus the enzyme activity can be conveniently determined in a one-step procedure if the enthalpy change is known for the reaction of interest.

If, however, the enzyme is present in large excess over the amount of substrate, the rate of formation of the product can frequently be described by:

$$d[P]/dt = \lambda_2[S] . \tag{18}$$

The power evolved is:

$$dq/dt = -\lambda_2[S]\, V\Delta H_6 . \tag{19}$$

The quantity λ_2 is a measure of the optimal rate of conversion of substrate(s) to product(s). Thus, a knowledge of the enthalpy change also allows one to conveniently determine the value of λ_2 from a microcalorimetric experiment. Application of this methodology to the assay of a sample of *glucose isomerase* is shown in figures 6 and 7.

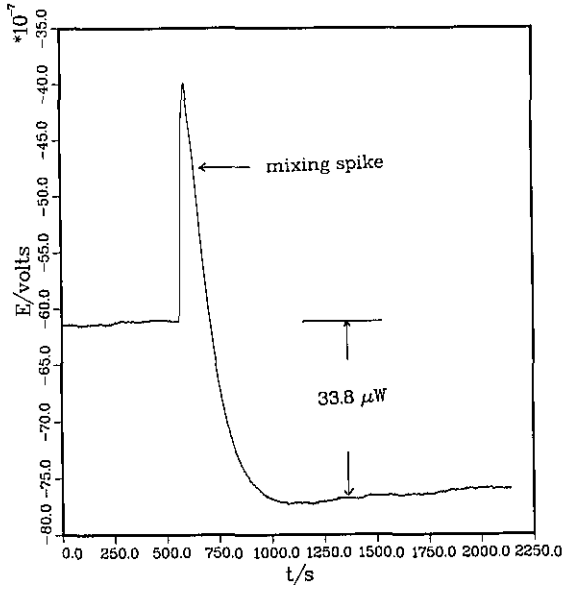

Figure 6–Microcalorimetric determination of the activity of a sample of *glucose isomerase*. The conditions of measurement were: T=50.0 °C, pH=7.4, and phosphate buffer (300.3 mM Na_2HPO_4 and 8.7 mM KH_2PO_4). The measured power was -33.8 μW and the amount of enzyme used was 25.8 mg of solution. Using this data and an enthalpy change of 4.68 kJ mol^{-1} [11] in equation (17) yields an activity of 2.8×10^{-7} mol s^{-1} (g solution)$^{-1}$ or 16.8 μmol min^{-1} (g solution)$^{-1}$. The deconvoluted curve is shown in the figure. Note that although there is a large mixing spike, it does not enter into the final measurement result.

We thank Edward Prosen for his helpful discussions on calorimetry and Irving Price and Nisan Altstein for their help with the electronic circuits.

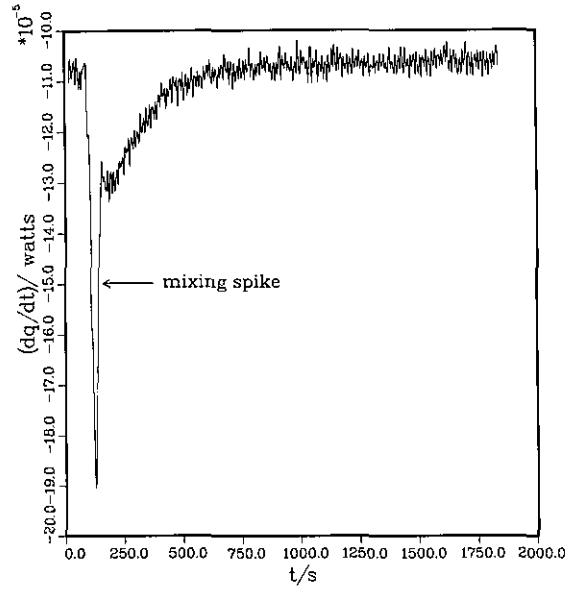

Figure 7–Microcalorimetric determination of the optimal rate of conversion of glucose to fructose using *glucose isomerase*. The conditions of measurement were: T=50.0 °C, pH=7.4, and phosphate buffer (30.3 mM Na_2HPO_4 and 8.7 mM KH_2PO_4). The initial concentration of the glucose was 4.02 mmol L^{-1}, and the total volume of solution present was 0.087 mL. The deconvoluted curve is shown in this figure. Extrapolation of the measured power to the start of the experiment yields a value of -42.0 μW. Use of this value, the initial concentration of the glucose, ΔH=4.68 kJ mol^{-1}, and eq. (19) leads to λ_2=0.0026 s^{-1}. As in the previous example (fig. 6), there is also a large mixing spike.

References

[1] Brown, H. D., ed., Biochemical Microcalorimetry, New York: Academic Press (1969).

[2] Beezer, A. E., ed., Biological Microcalorimetry, New York: Academic Press (1980).

[3] Prosen, E. J.; P. W. Brown, G. Frohnsdorff, and F. Davis, A Multichambered Microcalorimeter for the Investigation of Cement Hydration, Cement Concrete Res. **15**, 703 (1985).

[4] Steckler, D. K.; R. N. Goldberg, Y. B. Tewari, and T. J. Buckley, Computer Software for the Acquisition and Treatment of Calorimetric Data, NBS Technical Note 1224, in press.

[5] Prosen, E. J., Design and Construction of the NBS Clinical Microcalorimeter, NBS Report 73-179, Washington DC: Natl. Bur. Stand. (1973).

[6] Calvet, E., and H. Prat, Recent Progress in Microcalorimetry, edited and translated from the French by H. A. Skinner, New York: The MacMillan Company (1963).

[7] Ginnings, D. C., and E. D. West, Principles of Calorimetric Design, in Experimental Thermodynamics, Volume 1: Calorimetry of Non-Reacting Systems, J. P. McCullough and D. W. Scott, editors, London: Butterworths (1968).

[8] Brunetti, A. P.; E. J. Prosen, and R. N. Goldberg, J. Res. Natl. Bur. Stand. **77A**, 599 (1973).

[9] Goldberg, R. N., Thermodynamics of Hexokinase-Catalyzed Reactions. Biophys. Chem. **3**, 192 (1975).

[10] Goldberg, R. N., Thermodynamics of Hexokinase-Catalyzed Reactions. II. Measurement and calculation of enthalpies of reaction as a function of magnesium ion concentration. Biophys. Chem. **4**, 215 (1976).

[11] Tewari, Y. B., and R. N. Goldberg, Thermodynamics of the Conversion of Aqueous Glucose to Fructose. J. Solution Chem. **13**, 523 (1984).

[12] Tewari, Y. B.; D. K. Steckler, and R. N. Goldberg, Thermodynamics of the Conversion of Aqueous Xylose to Xylulose. Biophys. Chem. **22**, 181 (1985).

[13] Tewari, Y. B., and Goldberg, R. N., An Investigation of the Equilibria Between Aqueous Ribose, Ribulose, and Arabinose. Biophys. Chem. **22**, 197 (1985).

[14] Gajewski, E.; D. K. Steckler, and R. N. Goldberg, Thermodynamics of the Conversion of Fumarate to L-(-) Malate. Biophys. Chem. **22**, 187 (1985).

[15] Goldberg, R. N.; Gajewski, D. K. Steckler, and Y. B. Tewari, Thermodynamics of the Conversion of Aqueous L-Aspartic Acid to Fumaric Acid and Ammonia, Biophys. Chem., in press.

[16] Gajewski, E.; D. K. Steckler, and R. N. Goldberg, The Enthalpy of Hydrolysis of Adenosine 5'-triphosphate to Adenosine 5'-diphosphate, in review.

Journal of Research of the National Bureau of Standards

Standards Development For Differential Scanning Calorimetry

Volume 91 Number 3 May–June 1986

Jane E. Callanan, Sandra A. Sullivan, and Dominic F. Vecchia

National Bureau of Standards
Boulder, CO 80303

This article summarizes two studies made in preparation for standards development, by differential scanning calorimetry, for instruments such as scanning calorimeters, differential thermal analyzers, differential mechanical analyzers, and related thermal analysis devices. The first was an extensive study of the variability of differential scanning calorimeters when used for determining transition temperatures and enthalpies. The second was an evaluation of calibration procedures recommended by the American Society of Testing and Materials. These studies are described in detail in National Bureau of Standards Special Publication 260-*99*.

Key words: differential scanning calorimetry; fusion enthalpy; fusion temperature; pilot study; standards; thermal analysis; transition enthalpy; transition temperature.

Accepted: August 27, 1985.

Introduction

A need exists for a number of transition temperature standards for use with differential scanning calorimeters (DSCs), differential thermal analyzers (DTAs), and differential mechanical analyzers (DMAs). In addition, transition enthalpy standards are required for the DSC and DTA. Conventional calorimeters are absolute measuring instruments. Once such a calorimeter has been calibrated, the results obtained with it are thermodynamic values and remain so until the measuring system is altered. A repair to wiring within the measuring circuit, a change in the masses of various components of the calorimeter, or long-term aging and use effects necessitate recalibration. While the required time for the approach to equilibrium or shield behavior characteristics may depend on the nature of the specimen, the numerical results obtained do not as the system is an absolute measuring one.

On the other hand, most DSCs are not absolute measuring instruments; they require the use of standard substances to evaluate the correction factors, for both temperature and enthalpy, which must be applied in order to obtain corrected values for thermal properties.

The American Society for Testing and Materials (ASTM) recently issued revised calibration procedures for DSCs and DTAs [1,2][1]. Preliminary evaluations of these procedures in our laboratory showed them to be promising, particularly if the melting points of the fusion standards were spaced at 50–60 K intervals.

About the Authors: Jane E. Callanan and Sandra A. Sullivan are with the Center for Chemical Engineering in NBS' National Engineering Laboratory (NEL), while Dominic F. Vecchia is with NEL's Center for Applied Mathematics.

[1] Figures in brackets indicate literature references.

Existing temperature and enthalpy of fusion standards include six standard substances developed by the National Physical Laboratory (NPL), U.K. [3]. For these, temperatures have been determined in a triple-point cell; the enthalpies of fusion, in an adiabatic calorimeter.

A second group of substances, sponsored by the International Conference of Thermal Analysis (ICTA) in 1971, is available through the Office of Standard Reference Materials (OSRM) [4]. Theseare standards for temperature only; enthalpy values have not been reported. In addition, the uncertainty in the nominal values for the melting points cited for these latter substances is more than an order of magnitude greater than would be expected with more recent instrumentation. The cause of this uncertainty may lie in the substances themselves or it may be in techniques and instrumental factors associated with the initial measurements. Those measurements were intended for comparisons among instruments rather than for use as calibration standards.

A third set of reference materials, again only temperature standards, is also available from NPL. This consists of 10 organic compounds whose melting temperatures have been obtained in glass capillaries, at a heating rate of 2 K/min. The enthalpy of fusion standards have been selected from among these materials but were developed for different lots of material; thus the enthalpy values are not transferable.

For most reliable work with thermal analysis instruments it is desirable to have standards available that cover a range of temperatures, enthalpies and materials, e.g., metals, organic solids, inorganic solids, liquids, polymers, etc. [5].

Experience in our laboratory led us to believe that we might be able to develop satisfactory temperature and enthalpy standard reference materials for DSCs with a DSC. Accordingly, a variability study and a calibration study to evaluate the feasibility of such work were designed and undertaken. A brief description of these studies, and the results obtained, is presented here. These results indicate that the proposed procedures do allow for certification of standards satisfactory for use with DSCs, DTAs, and other thermal analysis instruments. A program of development of such standards has been undertaken at NBS–Boulder.

This article is intended to acquaint users of these instruments with the certification procedure. Full documentation and all data will be found in a cited NBS Special Publication [6].

Variability Study

To judge the suitability of a DSC for the development of standards, it is necessary to identify and evaluate the various sources of experimental variability in temperature and enthalpy measurements. In general, such variability could arise from the DSC, from the procedures and laboratory conditions for working with the DSC, or from inhomogeneity among specimens of the reference material. Studies to evaluate the effects of these sources of experimental error on the precision of DSC measurements are described in this section.

Three forms of indium (granules, rod, foil) were selected for this study. In the initial variability study, five specimens of each form were prepared and each specimen was run four times, remounting the specimens in the calorimeter between repeat measurements. The 20 measurements of temperature and enthalpy of transition on each form were obtained in random order over a long enough time period to include the effects of variations in line voltage, or other diurnal perturbations, on the results. Specimen masses varied from 0.93—3.49 mg; temperature and enthalpy of transition did not exhibit mass dependence in this range.

A statistical analysis was done (separately) on both temperature and enthalpy data for each form of indium. The analysis allowed for the possibility that large differences could exist between different specimens of the same indium form. Figures 1a and 1b illustrate the specimen-to-specimen (and within specimen) variability that can be seen in the data for granular indium. Variance calculations on the indium data describe both the internal variability of the measurements on a given specimen and the variability between sets of measurements on different specimens.

Both between-specimen and within-specimen components of variance were calculated in each analysis. The between-specimen component of variance is primarily associated with material variability of a given indium form. Hence, it provides a quantitative measure of inhomogeneity in the specimens with respect to temperature or enthalpy of transition. The within-specimen variance is that which occurs in the absence of sample inhomogeneity or when measuring a single specimen repeatedly. It contains contributions to overall variability other than specimen-related ones. With the present experimental design, these include instrumental factors and the effects of remounting the specimens, of operating procedures, and of ambient conditions.

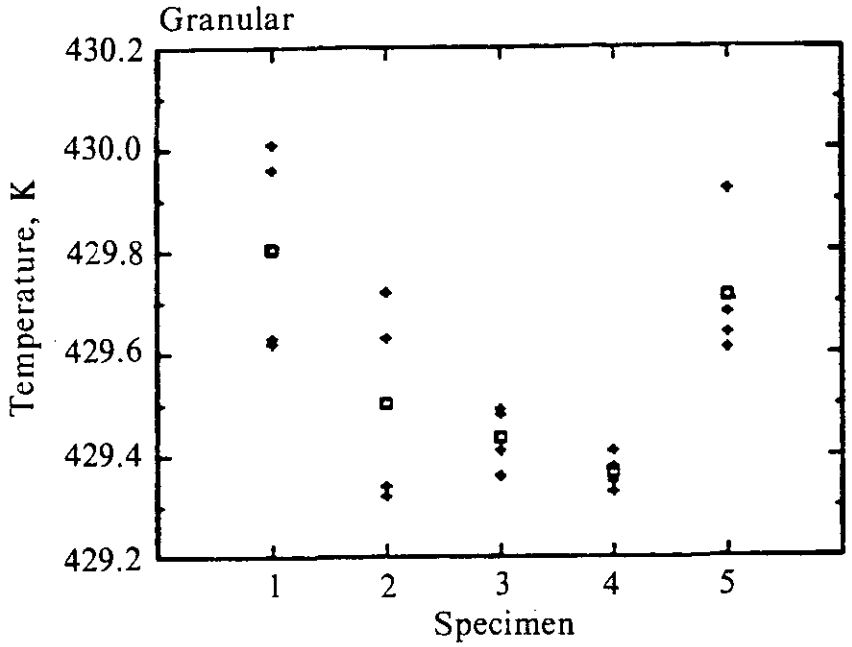

Figure 1a–Fusion temperature measurements for indium granules. (◘ indicates specimen mean)

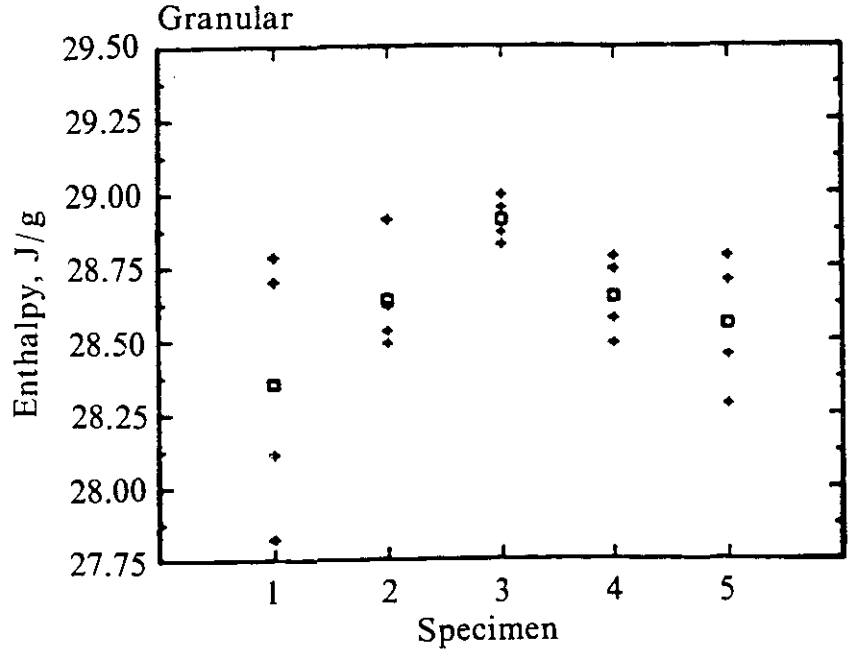

Figure 1b–Enthalpy measurements for indium granules. (◘ indicates specimen mean)

For measurements on a given form of indium, the within-specimen component of variance, S^2, and between-specimen component of variance, S_b^2, are calculated as follows:

$$S_b^2=\frac{1}{4}(4S_A^2-S^2)$$

and

$$S^2=\frac{1}{15}\sum_{i=1}^{5}\sum_{j=1}^{4}(X_{ij}-\bar{X}_i)^2 \qquad (1)$$

where

$$S_A^2=\frac{1}{4}\sum_{i=1}^{5}(\bar{X}_i-\bar{\bar{X}})^2.$$

In these formulae, X_{ij} denotes the j-th measured temperature (or enthalpy) on specimen i, $\bar{X}_i$ is the average of four values on specimen i, and $\bar{\bar{X}}$ is the grand average of all 20 values from 5 specimens.

Note that S^2 (15 degrees of freedom) is, in fact, the pooled within-specimen variance, commonly used by chemists,

$$S^2=\frac{1}{5}\sum_{i=1}^{5} S_i^2,$$

where S_i^2 is the usual estimated variance of the four repeat measurements on the i-th specimen. Thus, S^2 is a proper estimate for the (internal) variability of repeat measurements on a given specimen when there may be large differences between different specimens of an indium form. Also, S_A^2 is the estimated variance of specimen means, and in effect, reflects both between specimen variability and within specimen experimental errors. The formula for the between specimen component of variability, S_b^2, is obtained from standard statistical theory [7].

To obtain a realistic estimate of the standard error in the grand average $\bar{X}$, of all measurements on a given form of indium, the within specimen and between specimen components of variance are combined in the formula:

$$S^2(\bar{X})=\frac{S^2+4S_b^2}{20}. \qquad (2)$$

The average value, $\bar{\bar{X}}$, is an estimate of the average melting temperature (or enthalpy) of all specimens of a given form of indium, and eq (2) is the correct estimate of the standard error that should be used to assess the uncertainty in the average value. There are four degrees of freedom for $S^2(\bar{\bar{X}})$ in this analysis [7]. The average value, with its associated uncertainty, defines the limits within which investigators using the same material should expect their values to fall.

Estimates from this study of the average melting temperature and enthalpy of transition for each form of indium are given in table 1 and 2, respectively. Standard errors for these values were calculated using eq (2). Estimated standard deviations of repeat measurements on a single indium specimen are also given in the tables. These reported values were computed from the pooled within specimen variability using eq (1), because the usual formula for the standard deviation of all 20 measurements is inappropriate when there may be differences between sets of values from different specimens.

Estimates of the between-specimen component of variability of indium forms are given in table 3. A statistical test of the hypothesis of no specimen-to-specimen variability was computed in each analysis. Significance levels for the tests are reported in table 3. The levels that were attained show evidence of variation in melting temperature among specimens of granular indium, but no evidence of significant variation for either rod or foil. However, all three forms of indium exhibited possible inhomogeneity among specimens with respect to enthalpies of transition. Reasons for the apparent difference in properties of indium with respect to the two measured quantities are currently being investigated.

Because the initial study could not distinguish remount variability from variation due to the instrument itself, an additional six specimens (two of each form) were run three times in succession, with

Table 1. Mean temperatures obtained in indium standards study[1].

	Mean (K)	Standard Error (K)	Degrees of Freedom	Standard Deviation Among Repeats (K)	Degrees of Freedom
Granular	429.565	0.083	4	0.148	15
Rod	429.509	0.038	4	0.168	15
Foil	429.602	0.038	4	0.170	15

[1] See footnote, table 1.

Table 2. Mean enthalpies obtained in indium standards study[1].

	Mean (J/g)	Standard Error (J/g)	Degrees of Freedom	Standard Deviation Among Repeats (J/g)	Degrees of Freedom
Granular	28.623	0.089	4	0.256	15
Rod	28.761	0.105	4	0.270	15
Foil	28.936	0.055	4	0.148	15

[1] See footnote, table 1.

Table 3. Estimated specimen-to-specimen variation.

	Temperature		Enthalpy	
	Specimen-to-Specimen S_b^2	Significance Level, Test $\sigma_b=0$	Specimen-to-Specimen S_b^2	Significance Level, Test $\sigma_b=0$
Granular	$(0.171)^2$	0.0034	$(0.153)^2$	0.0937
Rod	0	0.5419	$(0.193)^2$	0.0502
Foil	0	0.7977	$(0.097)^2$	0.0692

no operator interference, to quantify the latter-source of experimental error. Additional studies allowed the evaluation of weighing error variation, effects of the computer analysis routine, and differences between operators. Estimates of the contributions to overall variability in DSC measurements from various sources of experimental variability are shown in table 4. (Only results for foil are given because the previous analysis shows foil measurements to be the preferred (i.e., less variable) form of indium for standards development.)

The results in table 4 were calculated in an ad hoc fashion from the combined results of the initial study and the additional data that were obtained later. Variation between operators is omitted from the table because operator differences were negligible. Errors introduced by the analytic procedure and specimen differences were negligible for temperature. They were not for enthalpy; in fact, specimen differences were the second most important component of the variance of the enthalpy. Variability introduced by the instrument itself, without contribution from remounting the specimen, was small in both instances. The most serious contributions to the variance of both temperature and enthalpy occurred as a result of replacing the specimens in the calorimeter.

Calibration Study

The second part of the study provided an evaluation of the temperature and enthalpy calibration procedures for DSC which have been recommended recently by the ASTM [1,2].

Table 4. Contributions to experimental variability (foil).

Source	Temperature Estimated Variance Component [K²]	Enthalpy Estimated Variance Component [(J/g)²]
Specimen	0	$(0.097)^2$
Analytic Procedure	0	$(0.055)^2$
Instrument	$(0.016)^2$	(0.023)2
Remount	$(0.169)^2$	$(0.136)^2$
Total	$(0.170)^2$	$(0.177)^2$

For temperature, the fusion temperatures for two well-characterized materials which bracket the temperature of interest were determined. The calculation of the observed transition temperature was obtained from

$$T=(TO\times S)+I, \tag{4}$$

where T is the corrected specimen temperature, TO is the observed temperature, S is the slope and I, the intercept. The slope and intercept are calculated from eqs (5) and (6).

$$S=(TS_1-TS_2)/(TO_1-TO_2)\,. \tag{5}$$

$$I=[(TO_1\times TS_2)-(TS_1\times TO_2)]/(TO_1-TO_2). \tag{6}$$

The TS_i are the literature values for the transition temperatures.

The associated enthalpies are corrected as follows. The transition enthalpy of a reference standard, usually indium, is measured and a calibration factor for the instrument determined at the transition temperature of this substance. The enthalpy correction is extended to other temperatures through use of a ratio of the heat capacity of a second standard, determined by the enthalpic method, at the reference temperature and at the temperature of interest. Sapphire is usually chosen for the second, heat capacity, standard because of its well-documented specific heat. The calibration coefficient (E) is obtained from the ratio of the literature value of the enthalpy of transition (ΔH_{lit}) to the observed value (ΔH_{obs}),

$$E=(\Delta H_{lit})/(\Delta H_{obs}). \tag{7}$$

Then the corrected enthalpy of fusion ΔH(corr) of measured specimens is obtained from

$$\Delta H(\text{corr})=E\times\Delta H(\text{meas}), \tag{8}$$

where ΔH(meas) is the measured enthalpy of fusion for that specimen. For extension to other temperatures a correction factor, F, is obtained from the results for the heat capacity of sapphire, Cp.

$$F = Cp(\text{lit})/Cp(\text{obs}) \quad (9)$$

The ΔH(corr) from eq (8) is multiplied by the ratio of the F-factor at the temperature of interest to the F-factor at the reference temperature. The F-factor normally changes somewhat with temperature; for that reason an F-factor specific to the temperature of interest is used.

The test materials selected were from the group of melting point standards certified by the NPL. The materials used and their reference temperatures are given in table 5.

Table 5. Melting points of test materials (K).

Substance	NPL Certificate Values [8]	Literature Values
Napthalene	353.37±0.05*	353.37 [9]
Acetanilide	387.51±0.05	387.51 [9]
Diphenylacetic Acid	420.41±0.05	420.41 [9]
Anisic Acid	456.45±0.2	456.14 [10]
2-Chloroanthraquinone	482.75±0.3	482.20 [10]

* Uncertainties represent one standard deviation.

The certificates for these materials indicate that these reference temperatures refer to a specific heating regime, heating at 2 K/min with the specimen contained in a glass capillary tube. Where other definitive work has been done, the values are listed in column 3 of table 5.

Five specimens of each of the five test materials were prepared; each was run four times. Randomly selected sets of the five substances were used and run in order of increasing temperature. Substances 1 and 3 were used, as bracketing substances, to calibrate the DSC and the transition properties of substance 2 were obtained. Then substances 2 and 4 were used for bracketing and the properties of substance 3 obtained. This procedure, followed through the selected list, would allow us to determine 1) whether the DSC would produce the accepted temperatures satisfactorily and 2) what error is to be expected in various temperature ranges.

The results, as given in table 6, separate the first run from the average of all four. Whether particular standards can be reused is always a question. Table 6 shows that, for the substances used here, differences between the first and the subsequent runs are of no practical significance. In those instances in which sample deterioration occurs, usually manifested by peak distortion, standard specimens cannot be reused.

Table 6. Summary of transition temperatures and enthalpies.

	Substance	Transition Temperature (K)	Enthalpy of Transition (J/g)*
INITIAL RUN			
	Naphthalene		149.35±0.85†
	Acetanilide	387.35±0.28†	163.65±1.26
	Diphenylacetic Acid	420.22±0.16	148.67±1.32
	Anisic Acid	456.18±0.41	195.49±0.76
	2-Chloroanthraquinone		148.15±0.76
ALL RUNS			
	Naphthalene		149.01±1.18
	Acetanilide	387.38±0.37	163.40±1.34
	Diphenylacetic Acid	420.23±0.39	148.16±1.28
	Anisic Acid	456.50±0.43	195.31±1.53
	2-Chloroanthraquinone		146.81±1.20
LITERATURE			
	Naphthalene	353.37 [9]	148.6 [9]
	Acetanilide	387.51 [9]	160.2 [9]
	Diphenylacetic Acid	420.41 [9]	147.3 [9]
	Anisic Acid	456.14 [8]	207.91 [8]
	2-Chloroanthraquinone	482.20 [8]	135.35 [8]

NOTE: Naphthalene and 2-chloroanthraquinone have no temperatures listed since they were the outer bracketing substances.

* The enthalpies of transition given are those that have been corrected by the fusion correction only (eqs. 4&5).
† Uncertainties represent one standard deviation.

The literature values quoted are for different lots of purified material from those used in this study or for results obtained by DSC in the early 1970s. Both DSC instruments and measuring techniques have improved greatly in the intervening years. Therefore, these results quoted here as literature values do not provide reliable criteria for comparison, but none more reliable are available currently.

Summary

The work reported here demonstrates that new standard reference materials for thermoanalytical instruments can be developed using the ASTM Recommended Practices [1,2]. The certified values for these materials will carry uncertainties in temperature an order of magnitude less than the ICTA standards presently in use. In addition they will be certified simultaneously for transition enthalpies. The best results are obtained when like substances are used for the calibrations and when the temperature difference between calibrants does not exceed 50 K. No blanket statement can be made about reusing standard specimens. If the fusion curves are not distorted, the specimen should be used again; if the curves are misshapen the specimen may not be reused.

It is anticipated that some of the materials that will be developed as standards, e.g., powders or crystals, will be readily homogenized. For these materials statistics which are appropriate for homogeneous materials, ungrouped data, will be applied. For materials which exhibit some inhomogeneity, as did some of the metallic samples used in this study, a statistical model which can separate the effects of inhomogeneity from other factors will be applied.

The results of this study, summarized here, make the use of a DSC for the development of fusion standards for the broad class of thermal analytical instruments creditable. A long-range program for the development of such standards is underway in this laboratory.

The authors thank Keith R. Eberhardt of the Center of Applied Mathematics, National Bureau of Standards–Gaithersburg for helpful advice and discussion concerning this study and the manuscript.

References

[1] ASTM Standard Practice for temperature calibration of differential scanning calorimeters and differential thermal analyzers E967-83. Annual Book of Standards. 14.02: 782-787 (1984).

[2] ASTM Standard Practice for heat flow calibration of differential scanning calorimeters E968-83. Annual Book of Standards. 14.02: 788-794 (1984).

[3] NPL Certified Reference Materials and Transfer Standards. National Physical Laboratory, Teddington, U.K. (1982 July).

[4] Office of Standard Reference Materials, National Bureau of Standards, Gaithersburg, MD 20899.

[5] Flynn, J. H., Theory of differential scanning calorimetry coupling of electronic and thermal steps, in Analytical Calorimetry, Vol. 3, R. S. Porter and J. F. Johnson, eds. New York, NY: Plenum Press, 17–44 (1974).

[6] Callanan, J. E.; S. A. Sullivan, and D. F. Vecchia, Feasibility study for the development of standards using differential scanning calorimetry. National Bureau of Standards (U.S.) Spec. Publ. 260-99 (1985 May).

[7] Box, G. E. P.; W. G. Hunter, and J. S. Hunter, *Statistics for Experimenters*, New York: John Wiley, 571–583 (1978).

[8] NPL Certificate of measurement CRM No. M14-11. Set of ten melting point standards. National Physical Laboratory, Teddington, U.K. (1980 November).

[9] Andon, R. J. L., and J. E. Connett, Calibrants for thermal analysis. Measurement of their enthalpies of fusion by adiabatic calorimetry. Thermochimica Acta **42**: 241–247 (1980).

[10] Pella, E., and M. Nebuloni, Temperature measurements with a differential calorimeter. Journal of Therm. Anal. 3: 229–246 (1971).

Journal of Research of the National Bureau of Standards

Miniature Mercury Contact Switches For Instrument Temperature Control

Volume 91 Number 3 May–June 1986

Thomas J. Bruno and Jerry G. Shepherd

National Bureau of Standards
Boulder, CO 80303

In this short note, we describe the design and construction of several modifications of miniature mercury contact switches for use in laboratory temperature control applications. Commercial contact switches, or contact thermometers as they are commonly called, are limited in their application because of their large size. The units which we present here are much more compact and are thus suitable for a wider range of applications. The limitations of the miniature contact switches in their present configurations are also discussed.

Key words: contact switch; contact thermometer; temperature controllers.

Accepted: September 17, 1985

1. Introduction

Temperature control for the components of laboratory instrumentation is achieved in a variety of ways. Depending on the level of accuracy required, contact switches, thermocouples, thermistors, and resistance devices are commonly used to control the power applied to heaters [1,2][1]. Thermistors and resistance devices are well suited to proportional control of the power input. Contact switches and thermocouples are easily applied to bipolar (on/off) control of heating elements.

All of these devices have their inherent limitations. For example, thermistors are usually limited to a maximum working temperature of 150 °C (423 K). Thermo-couples are subject to aging effects and become brittle and difficult to handle after operation at high temperature. The control circuitry associated with the use of thermistors and resistance devices is relatively expensive. Mercury contact switches (contact thermometers) have been used extensively for the control of stirred liquid bath temperature. The circuitry required for these simple on/off switches is inexpensive relay devices, which can control temperature with a precision approaching ±0.005 K [3]. The large size and heat capacity of commercial mercury contact switches have limited their use in most other applications.

About the Authors: Thomas J. Bruno and Jerry G. Shepherd are with the Thermophysics Division in the NBS National Engineering Laboratory. The work they describe was supported by the Gas Research Institute and the Department of Energy.

[1] Figures in brackets indicate literature references.

2. Discussion

In order to overcome some of these physical limitations and apply the contact switch to the 400 to 575 K region, we have designed and fabricated several miniature, high sensitivity fixed and adjustable mercury contact switches. These are shown in figure 1. The units labeled a and b are fixed contact

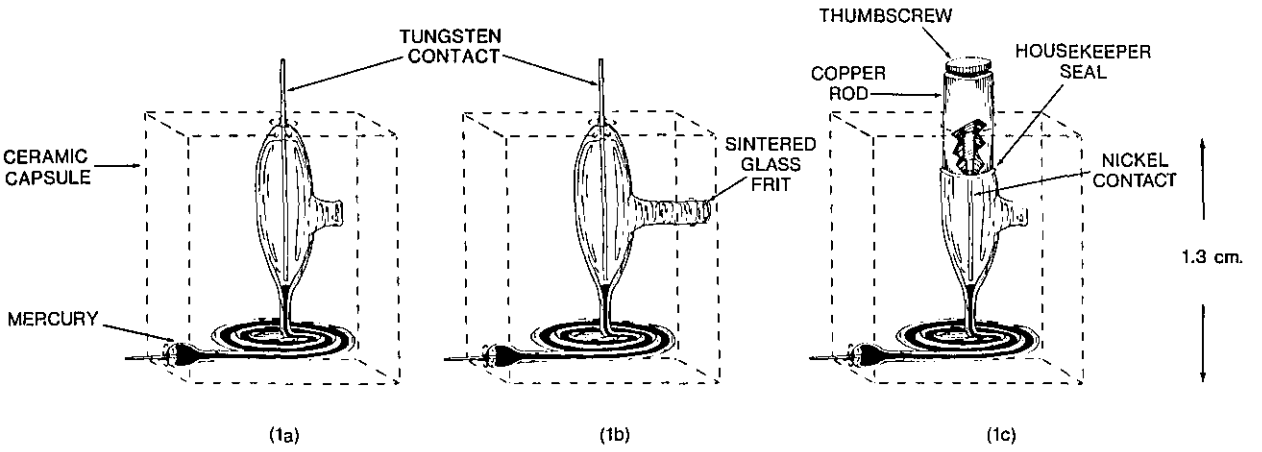

Figure 1–The sealed, evacuated contact switch, a); ambient temperature modification of the switch, b); and the adjustable temperature switch, c).

switches which will regulate at a single specific temperature that must be set during fabrication. The body of each switch is made from borosilicate glass tubing (5 cm long, of 1.0 mm o.d. and 0.2 mm i.d.), and utilizes tungsten contacts.

The bulbs at either contact were made from uranium glass, in order to grade the seal to the tungsten. The switch shown in 1a is sealed under vacuum (10^{-7} MPa) and is suitable for use at elevated temperature. The upper bulb serves as an expansion reservoir, to prevent the unit from shattering in the unlikely event of a large temperature overshoot or a circuit failure. The unit shown in 1b is a lower temperature modification of the fixed contact switch. The upper bulb is not evacuated, but is open to atmospheric pressure via a sintered glass frit.

With an adjustable contact switch as shown in 1c, the upper contact may be lowered or raised using the thumbscrew. The screw threads are covered with a commercial mixture of colloidal copper in vacuum grease, which lubricates the threads and insures good electrical contact. Since this switch is not sealed, its use is confined to lower temperature applications.

In practice, the contact switch is potted in a small pellet of a specially formulated aluminum-silicon oxide ceramic [4]. Alternatively, a high temperature silicone elastomer-aluminum mixture can be used. This pot provides good heat conduction and makes the switch more durable. This is desirable since the glass tubing is quite fragile.

The contact switch shown in figure 1a has been used to control the temperature of a chromatographic sampling system at 400 K [4,5]. In this temperature region, the performance of thermistor based temperature controllers can be marginal. The contact switch is sensitive to changes in temperature on the order of 0.05 K. The circuit (which responds to the contact switch) required to supply power to the heating elements is a simple solid state relay, shown in figure 2 [6].

The usefulness of these switches as substitutes for commercial mercury contact switches stems from the compactness of their design. They can be incorporated easily into instrument components which could not accommodate a larger commercial unit and where the use of a thermistor would provide marginal performance. The principal limitation of the switch in its present configuration is the inability to adjust the set point of the evacuated switch once the upper bulb is sealed. Thus, a separate switch is needed for each desired set point. This is not a serious problem for operations involving long term isothermal operation, but an adjustable sealed unit would be useful. Modifications along these lines are currently being pursued.

3. References

[1] Quin, T. J., Temperature, Academic Press, London (1983).

[2] Vassos, B. H., and G. W. Ewing, Analog and Digital Electronics for Scientists, New York: John Wiley and Sons (1980).

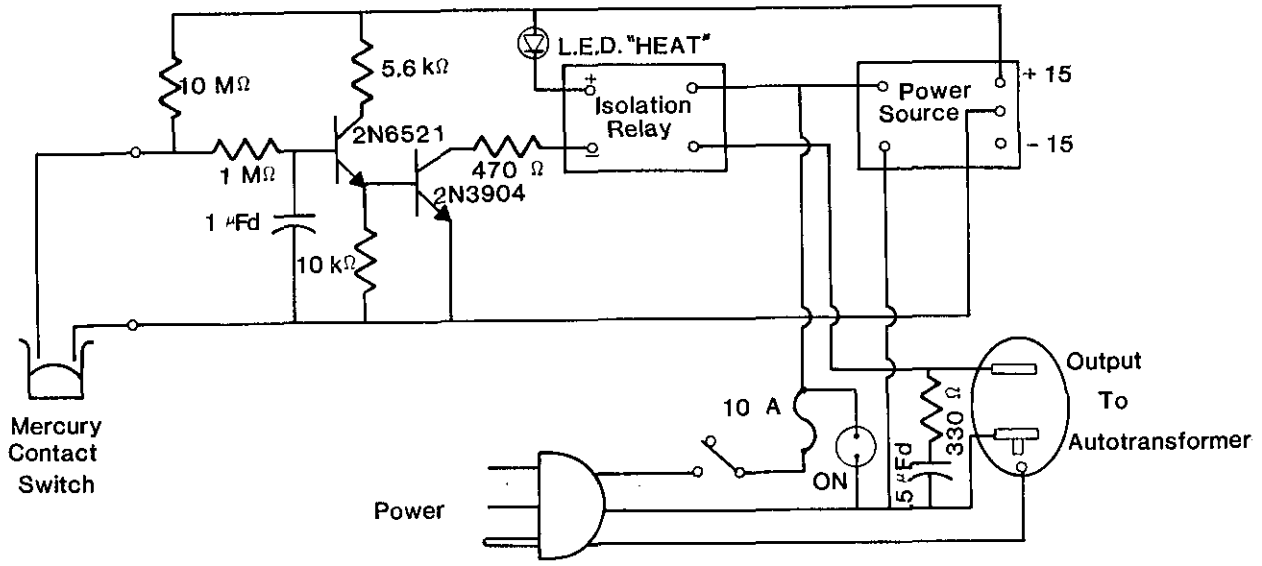

Figure 2–Circuit diagram for a simple solid state relay for use with the contact switches.

[3] Bruno, T. J.; D. E. Martire, M. W. P. Harbison, A. Nikolic, and C. F. Hammer, J. Phys. Chem. **87**, 2425 (1983).
[4] Bruno, T. J., J. Chromatogr. Sci. **23**, 325 (1985).
[5] Bruno, T. J., J. Res. Natl. Bur. Stand. (U.S.) **90**, 127 (1985).
[6] Frederick, N. V., and J. McFarlane, Private Communication (1985).

Journal of Research of the National Bureau of Standards

Thermophysical Property Measurement on Chemically Reacting Systems—a Case Study

Volume 91 Number 3 May–June 1986

Thomas J. Bruno and Gerald C. Straty

National Bureau of Standards
Boulder, CO 80303

This short paper describes several experimental approaches for dealing with chemical reactions or decomposition which can occur when making thermophysical property measurements at high temperature and high pressure. The associated equipment was designed and built to allow thermophysical property data to be cast in a more realistic perspective by taking explicit account of chemical changes which may occur during an experiment. As an example of these methods, the measurements on the methanol system are discussed in detail.

Key words: chemically reacting systems; decomposition; high temperature; methanol; thermophysical properties.

Accepted: November 18, 1985

1. Introduction

Recent work on the PVT (pressure-volume-temperature) [1][1] and VLE (vapor-liquid equilibrium) properties [2] of methanol at high temperature and high pressure has demonstrated the need to take explicit account of the possibility of chemical reactions occurring during thermophysical property measurements [3]. The major factors which govern these reactions are the result of thermodynamic, kinetic, and catalytic effects. Thermodynamic factors include activation energies and equilibrium positions. The primary kinetic consideration is the strong temperature and density (concentration) dependence of the rate constant. The experimental apparatus itself may contribute significantly to chemical reactions by serving as a catalytic agent. While it is clear that the measurement apparatus may be the major factor in fluid decomposition [4], it is equally clear that it will not be possible to build a separate instrument for each fluid. We have therefore designed and applied several sampling and pilot simulation systems to conventional analytical instrumentation in order to assess the extent of chemical react or decomposition which might be expected in a measurement system. In this short paper, we will describe some of these techniques and discuss the measurements on the methanol system as an example of their use.

About the Authors: Thomas J. Bruno and Gerald C. Straty are with the Thermophysics Division, part of NBS' National Engineering Laboratory. The work they describe was supported by the Department of Energy, Office of Basic Energy Sciences.

[1] Figures in brackets indicate literature references.

2. Experimental

The principal experimental apparatus for reaction screening in conjunction with thermophysical property measurement is a laboratory scale batch-semibatch reactor. This reaction screening apparatus is shown schematically in figure 1, and is described fully elsewhere [5]. The heart of the apparatus is a small, thick walled pressure vessel

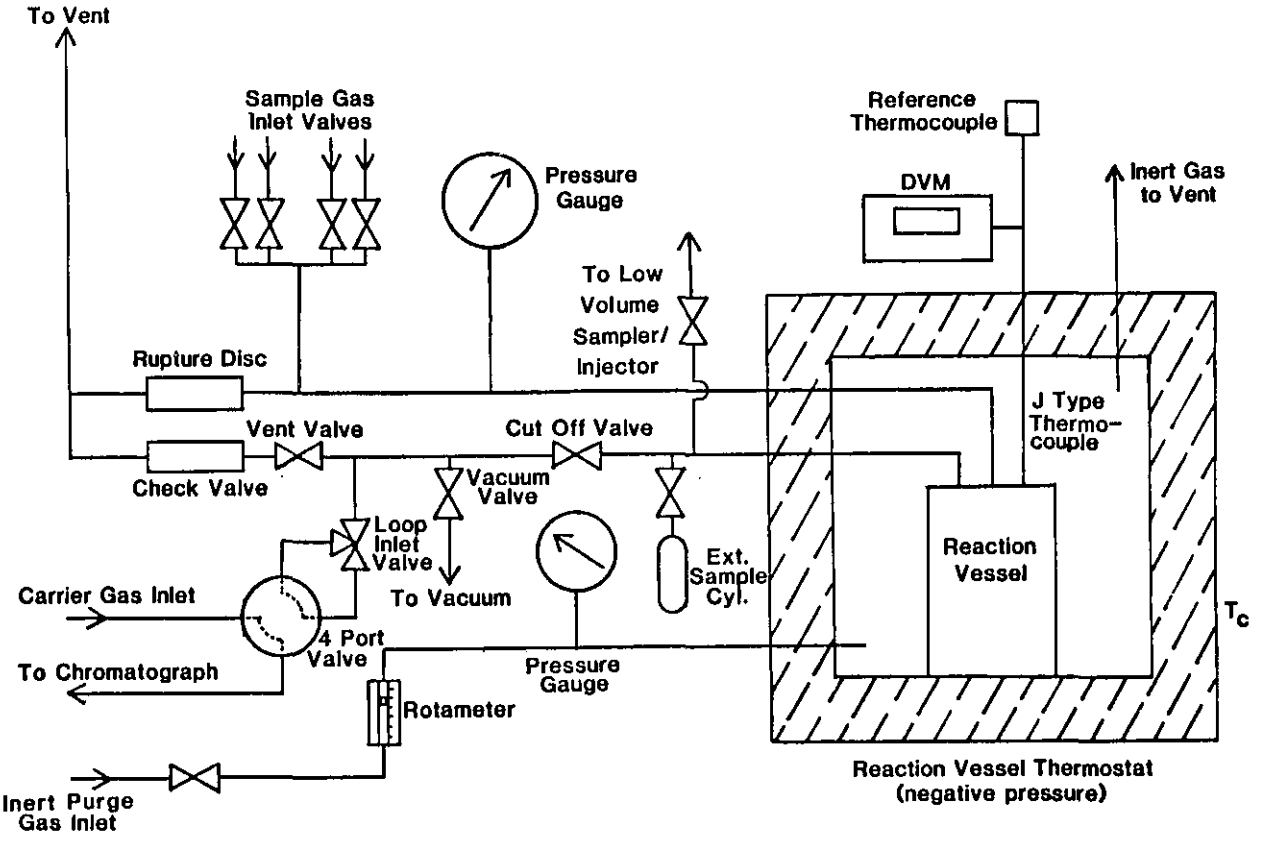

Figure 1–Laboratory scale batch-semibatch reactor.

(316L stainless steel). The vessel incorporates a bolted closure which is sealed using either a 25% glass filled PTFE gasket (for temperatures up to 240 °C) or a 316L stainless steel gasket (for temperatures as high as 450 °C). At 250 °C, the vessel can safely contain a pressure of 130 MPa [6]. The vessel is contained within a specially constructed oven which is maintained at a slight negative pressure gradient (using an air or water transvector) during operation.

Sampling and analysis of the contents of the pressure vessel can be done in several ways during the course of a screening test. The sample line is connected to a modified chromatographic four-port sampling valve which is in turn connected to an analytical chromatograph. This chromatograph is equipped with an ultrasonic (sound velocity) detector, and is primarily used for gas analysis. Alternatively, sample may be collected in a sampling cylinder (which may be quenched in liquid nitrogen) for off-line analysis. This makes possible the use of mass spectroscopy and spectrophotometry, as well as more specific tests.

An additional option for chromatographic analysis of the vessel contents is the use of a low volume sampler-injector. This apparatus, which is shown schematically in figure 2, is fully described elsewhere [7]. In practice, this injector is installed in place of the external sampling cylinder which is shown in figure 1. This device allows the manipulation and injection of small volumes of gaseous samples, which is advantageous when hazardous materials may be involved. The precision that is possible with this injector is far better than that obtainable with commercial injectors that depend upon the use of relatively large sample volumes in order to achieve a reasonable degree of precision.

As a rough indication of the catalytic effect (and nominal temperature dependence) of wetted surfaces inside a measurement apparatus, reaction chromatography is often useful. In this technique, a bed of granular or powdered material precedes the separation column. This bed is composed of the material that makes up the construction of the measurement apparatus and is maintained at the same temperature as the separation column. It is then possible in a gross manner to determine the onset temperature of chemical decomposition or polymerization. One can then identify reaction products using mass selective detection (mass spectroscopy) or by comparison of the retention times of injected standards. There are a number of drawbacks to this technique, and it therefore must

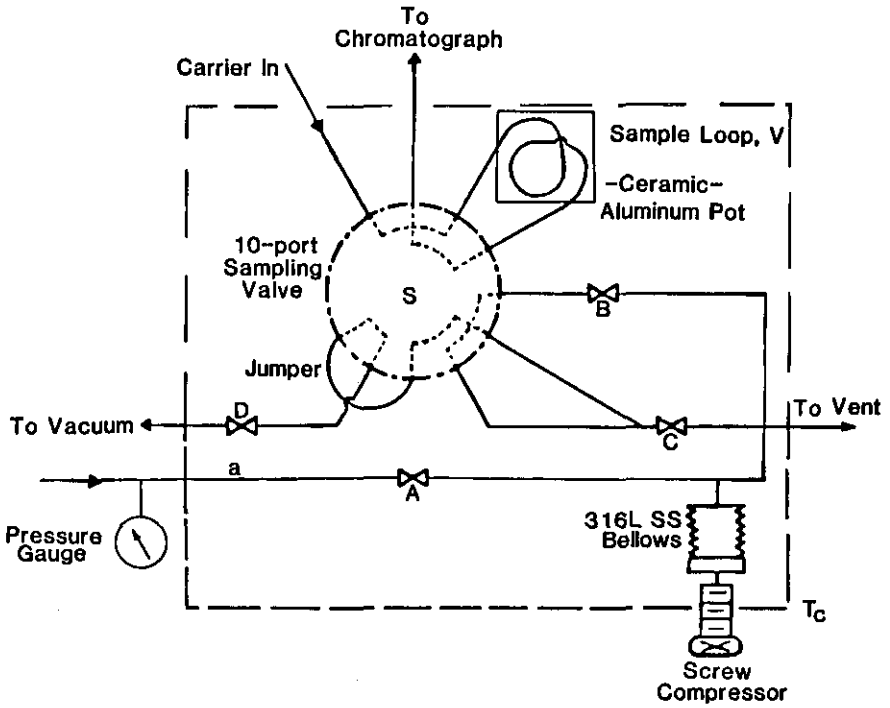

Figure 2–Low volume sampler-injector

be used with great care. The chromatographic column is normally operated at low pressure, and the sample is diluted by the carrier gas. In addition, the ratio of the sample mass to surface area (of the bed material) is essentially uncontrollable. It is therefore unreasonable to expect exact duplication of the conditions in a PVT or VLE apparatus. From a chromatographic point of view, the use of the bed with capillary columns is inconvenient. This problem is of little consequence when the analyte is gaseous or volatile, since packed columns (especially porous polymer packings) will perform very well. As the temperature of the bed and separation column is increased during the course of a screening test, the carrier gas flow rate will need to be reduced. This change in flow will limit quantitative accuracy to no better than 2 percent, regardless of the method of detection and calibration employed.

In addition to the methodology applied to gas chromatography, liquid chromatography and infrared and ultraviolet spectrophotometry have found some use in reaction screening for thermophysical property measurements. The inherently lower efficiency of liquid chromatography and the need to make the transition from the high temperature region to essentially ambient temperature have limited its usefulness in this application. Infrared spectrophotometry (IR) can often provide valuable information, especially on simple, one component systems such as methanol or benzene [1,8]. The spectra are measured on samples collected from the reactor (fig. 1) or directly from the PVT or VLE apparatus. It is often the case that IR will provide useful negative information; knowledge of functional groups that are absent is almost as helpful as knowledge of what is present. Ultravoilet spectrophotometry is employed in the same way as IR, except that the functional group information is far more limited than that provided by IR.

3. Results—Methanol

As mentioned earlier, PVT and VLE studies on pure methanol indicated substantial chemical reaction occurring at temperatures near and above 200 °C. The liquid phase withdrawn (at ambient temperature and pressure) from a high temperature VLE cell [2] was found to be in equilibrium with a significantly large vapor phase fraction. The liquid itself had a strongly rancid odor. The same odor was noted upon withdrawal of methanol from the high temperature PVT apparatus [1] after the methanol was exposed to temperatures in excess of 200 °C. In addition, a measurable residual pressure (due to a gaseous phase) was noted upon condensation of the liquid methanol from the PVT cell using a liquid nitrogen cold trap. This indicated the probable presence of hydrogen and/or carbon

monoxide in the residual gas.

A number of studies involving the techniques described earlier were initiated in order to cast the PVT and VLE measurements in a more useful perspective. An aliquot of methanol was maintained at 250 °C and 3.7 mPa for 48 hours using the apparatus shown in figure 1. Analysis of the gaseous phase (by gas chromatography) after cooling indicated the presence of both hydrogen and carbon monoxide. The liquid phase was found to have the same rancid odor noted previously. Infrared spectrophotometry indicated the presence of an ether linkage in an impurity species present in the liquid. This was confirmed by mass spectrometry, which indicated the presence of dimethylether. Gas chromatographic analysis of the liquid indicated the presence of formaldehyde, and several heavier impurities which could not be identified by their mass spectra alone. Testing the liquid with acidified 2,4-dinitrophenylhydrazine confirmed the presence of formaldehyde by the identification of the red precipitate of the 2,4-dinitrophenylhydrazone. The acidic mother liquor developed further precipitate upon standing, indicating the presence of acetals and hemiacetals [10], which probably make up the heavier impurities found on the chromatogram.

In order to ascertain the catalytic behavior of the 316L stainless steel PVT cell, and to estimate the nominal temperature dependence of the reaction rate and product distribution at elevated temperatures, the reaction chromatography technique described earlier was used. In this approach, a 1.5 m long, 0.6 cm o.d. stainless steel column was almost completely filled whith Chromosorb 102[2], with the final 5 cm at the column inlet being made up with powdered 316L stainless steel. Injected samples of pure methanol then pass over the bed of powdered stainless steel before the resulting sample plug is applied to the separation column. Example results from this study are given in table 1, along with data taken on a column differing only in the absence of the powdered stainless steel bed. The area percent measurements were made using helium carrier gas and thermal conductivity detection. The flow rate was decreased as the temperature was increased; thus the reported percent compositions of light (more volatile than methanol) and heavy (less volatile than methanol) reaction products are only approximate. Serious decomposition/reaction problems are seen to begin at 200 °C, and become extremely severe at 250 °C. Hydrogen was produced at a temperature between 210 and 225 °C. Carbon monoxide, another highly probable product at this temperature, could not be resolved from the methanol peak.

Table 1

Temperature °C	Area Percent Methanol	Area Percent Light Impurities	Area Percent Heavy Impurities
	REACTION COLUMN		
100	99.8	0.2	0
200	95.2	1.0	3.8
250	85.7	0.3	14.0
	CONTROL COLUMN		
100	100	0	0
200	100	0	0
250	100	0	0

The results discussed above are in general agreement with earlier observations [4]. Analyses done on each methanol charge in the PVT experiment yielded results which were expected on the basis of these reaction screening studies. Corrections were made to the PVT data of methanol on the basis of these studies of the onset of reactions, and are fully described elsewhere [1].

[2] Certain commercial equipment, instruments, or materials are identified in this paper in order to adequately specify the experimental procedure. Such identification does not imply recommendation or endorsement by the National Bureau of Standards, nor does it imply that the materials or equipment identified are necessarily the best available for the purpose.

4. References

[1] Straty, G. C.; A. M. F. Palavra and T. J. Bruno, PVT properties of methanol at temperatures to 300 °C, Int. J. Thermophys. (in press).

[2] Mayrath, J. E. (in preparation).

[3] Hanley, H. J. M., Position statement on chemically reactioning systems (a copy of which may be obtained via personal communication with the author of this paper) (1984).

[4] Ta'ani, R. Doctoral Dissertation, Karlsruhe University (1976).

[5] Bruno, T. J., and G. L. Hume, A high temperature, high pressure reaction screening apparatus, J. Res. Natl. Bur. Stand. (U.S.), **90** (3), 255 (1985).

[6] ASME Boiler and Pressure Vessel Code, Sec. VIII: Unfired Pressure Vessels. New York: American Society of Mechanical Engineers (1965).

[7] Bruno, T. J., A simple gas sampling and injection apparatus. J. Chromatogr. Sci. **23**, 325 (1985).

[8] Straty, G. C.; M. J. Ball and T. J. Bruno, PVT properties of benzene at temperatures to 450 °C, Int. J. Thermophys. (in preparation).

[9] Straty, G. C., and A. M. F. Palavra, Automated high-temperature PVT apparatus with data for propane, J. Res. Natl. Bur. Stand. (U.S.) **89** (5), 375 (1984).

[10] Svoronos, P. D. N., City University of New York, Bayside, NY, 11364, private communication (1984).

Journal of Research of the National Bureau of Standards

Inorganic Materials Biotechnology: A New Industrial Measurement Challenge

Volume 91 Number 3 May–June 1986

G. J. Olson and F. E. Brinckman

National Bureau of Standards
Gaithersburg, MD 20899

Biotechnological processing of inorganic, heavy elements has only begun to emerge as we start to understand microbial strategies and mechanisms of heavy element transformations. Chemical speciation of key, diagnostic intermediates and products of bioprocessing in gas, liquid, and cellular phases, and on surfaces, is required to understand and optimize important reactions. Recent discoveries of microorganisms in metal-enriched thermal environments, and further investigations into production of exocellular metal transforming metabolites, offer exciting prospects for development of new technologies for strategic and precious materials recovery and processing.

Key words: biotechnology; chemical speciation; chromatography; element-specific imaging; epifluorescence microscopy; inorganic materials; metallophilic bacteria; metals bioaccumulation; ore bioprocessing; organometals; strategic metals; thermophilic leaching.

Accepted: December 5, 1985

1. Introduction

1.1 Inorganic Materials Biotechnology—Its Roots and Potential

Among the oldest of man's technologies, biotechnology has lately captured scientific, commercial, and public attention for the wide scope of organic materials such as pharmaceuticals, foodstuffs, or commodity chemicals, and improved energy economies, it presages. Basically, biotechnology "... involves the use of living organisms to make commercial products and includes three major areas of research effort: recombinant DNA methodology, monoclonal antibody techniques, and bioprocessing ..." [1][1]. The recent challenges and opportunities perceived for biotechnology depend upon a clear and reliable measurement base at the level of molecular biology, and hence increasingly must involve novel contributions from many chemical disciplines as well.

Not so familiar to casual onlookers and non-specialists is the fact that biotechnology deals with or more than organic materials comprised of a few light elements such as carbon, hydrogen, oxygen, nitrogen, sulfur and phosphorus; it deals with the majority of the remaining 90-odd elements that also influence our biosphere. However, inorganic materials bioprocessing is receiving attention from many industries where microorganisms are increasingly perceived as potential low-energy routes to recovering metals from ores, upgrading of ores and fossil fuels prior to conventional processing and combustion, and toxic and/or precious metal precipitation and recovery in waste streams. The po-

About the Authors: G. J. Olson and F. E. Brinckman are with the Ceramics Division of NBS' Institute for Materials Science and Engineering. The work they describe was supported in part by the Office of Naval Research.

[1] Figures in brackets indicate literature references.

tential of this biotechnology was addressed by academic, government, and industrial representatives at the recent Workshop on Biotechnology for Mining, Metal-Refining and Fossil Fuel Processing Industries [2] at Rensselaer Polytechnic Institute, Troy, NY (May 28–30, 1985). It is now clear that major sectors in North American mining technologies are moving rapidly to further develop biotechnological processing, including, for example CANMET (Canada Centre for Mineral and Energy Technology) [2] and the participation of the U.S. National Laboratories investigating "leapfrog" technologies for the steel industry [3]. One such technology would be bioprocessing of iron ores for removal of impurities or waste bioprocessing.

Investigations into the range and potential for commercial microbial transformations of heavy elements are just beginning. This paper therefore emphasizes inorganic bioprocessing, its industrial potential, and the measurements needed to characterize, monitor, and apply the inorganic reactions that microorganisms perform.

1.2 Environmental Perspective of Inorganic Materials Biotechnology

The lighter "organic" molecule-forming elements (C,H,O,N,S,P) make up the bulk of cell constituents and thus are essential nutrients for cells. However, many "inorganic" or heavy elements, including both metals and metalloids are essential in biological processes, often as enzyme cofactors, but in some cases as energy sources and electron acceptors in respiration [4]. Still other heavy elements are toxic and have no known metabolic function, such as Hg or Cd. Organisms which detoxify (by oxidizing, reducing, complexing, alkylating) these elements are often found associated with metal ore deposits, industrial waste discharges and other special and unusual environmental sites including, geothermal springs in terrestrial volcanic locales or geothermal sea-floor vents recently reported at great ocean depths [5]. Unexpectedly rich growths of microorganisms isolated from these metal-rich regions display capacities for heavy metal transformations even at high temperatures and pressures, implying tremendous possibilities for bioprocessing.

Microbial processing of metals and metalloids also occurs in less severe environments as evidenced by the burgeoning literature describing natural biotransformations of many elements [4]. At this point, our state of knowledge is incomplete regarding the range of beneficial as well as inimical transformations of many heavy elements. From an environmental viewpoint, this issue is, and must remain, a vital R&D component of monitoring and regulation. For example, the public health disasters in Japan two decades ago resulting from "Minimata Disease," or methylmercury poisoning, of a general seacoast population eating contaminated fish were exacerbated by underlying chemical and bacterial transformations of industrial mercury discharges into marine sediments and subsequent transmission into food webs [6]. Nonetheless, the same basic understanding of metals biotransformations and the related measurement methodology also supports promising new ventures in "inorganic" biotechnology.

Following the Minimata disaster, work in many laboratories, including ours at NBS, showed the prevalence of environmental mobilization by biotransformations of mercury and other heavy elements in polluted sediments [6]. Recent reports show that microorganisms may possess metal-induced resistance to metals and antibiotics [7,8]. Several elements besides mercury have been implicated in this way, including arsenic [9], silver [10], and cadmium [11]. Hence, applications of such results growing out of environmental and health research bears equally great promise for inorganic bioprocessing designs and applications.

1.3 Mechanisms of Metals Biotransformations

Since extra-chromosomal components of bacteria, called plasmids, have been demonstrated to confer new enzymatic capabilities in cells for highly effective metal- and metalloid-processing [12], and these plasmids can be genetically manipulated within current biotechnology, the earlier information on environmental impacts of such elements may now find new utility in the design and application of genetically-modified bacteria capable of industrially important processes. Plasmid mediated metal transformation often serve to detoxify metals. However, some microorganisms enzymatically oxidize heavy elements such as Fe(II), Sb(III), or U(IV) as energy sources. In certain bacteria, electrons from these reduced metals are passed to various electron acceptors spanning the cytoplasmic membrane. This generates a proton motive force across the membrane which drives ADP phosphorylation to ATP [13]. Table 1 summarizes a number of reactions for those microorganisms thus far studied and offers two examples of potential energy sources, but it should be regarded in light of the vast potential for useful reactions of many other heavy elements thus far unexplored.

Table 1. Examples of heavy elements used as energy sources by bacteria.

Metal Bioprocess	Terminal e^- Acceptor	Organism	Ref.
$Fe^{2+} \rightarrow Fe^{3+}$	O_2	*T. ferrooxidans*	13
$Sb^{3+} \rightarrow Sb^{5+}$	O_2	*S. senarmontii*	14
$U^{4+} \rightarrow U^{6+}$	O_2	*T. ferrooxidans*	15
$Cu^{+} \rightarrow Cu^{2+}$	O_2	*T. ferrooxidans*	16
Examples of reactions that potentially yield enough energy for ATP synthesis, but not yet demonstrated with organisms.			
$Co^{2+} \rightarrow Co^{3+}$	O_2		17
$As^{3+} \rightarrow As^{5+}$	O_2		18

The paucity of knowledge of such "inorganic" biochemistry has and will remain subject to progress with measurement state of art. Reliable methods for characterization of microbial metal transforming processes are needed both for understanding mechanisms and, ultimately, for process monitoring in the commercialization of such element-transforming processes [19].

2. Measurement Requirements and Prospects for Inorganic Materials Biotechnologies

Though not widely described, there already exists in the United States and elsewhere industrial use or practical demonstrations of microbial processing of metal ores *in situ* and sequestering of heavy metals from waste streams. Table 2 provides examples in recent use along with the key metal products. The translation of laboratory demonstration to cost-effective field processing will largely depend upon the reliability and sensitivity of real-time monitoring, as well as the measurement capa bility for element-specific quantitation. Where field use is already practiced, effects of potential rate limiting toxicants and means for process optimization have yet to be fully investigated. Future developments will also likely include bioprocessing of ore concentrates under controlled conditions. In such processes, container materials must withstand corrosive biogenic agents and possibly elevated temperatures and pressures.

Table 2. Examples of commercial applications of metals bioprocessing.

Application	Industry	Metal Product	Ref.
Ore leaching			
Cu	Mines in W. USA	Cu^{2+}	20
U	Mines in Canada, USA	U^{6+}	21
Total metal precipitation			
Pb, Zn	Mines in Missouri	oxides, sulfides	22
U*	Nuclear waste effluents	UO_2^{2+}	23
Precious metal recovery			
Ag*	Photographic effluents	Ag^o	24
Ag, Au*	Pyritic gold, silver ores	Ag^o, Au^o	25

* Laboratory scale investigations for feasibility of bioprocessing.

2.1 Process Options

Experience in inorganic bioprocessing to date indicates [26] that three major separate or concerted routes are effective in transforming, isolating, and concentrating desired heavy elements. These are: 1) chemomechanical separation and concentration; 2) solubilization (and redox); and 3) direct cellular uptake or accumulation.

2.1.1 Surface Pretreatments Using Biomodification. Fossil fuel upgrading employing microbial cell cultures has been used to remove pyritic sulfur, that is iron sulfide constituents, from coals either by direct solubilization of the mineral component [20], or by rendering the pyrite hydrophilic through biotransformation followed by oil agglomeration [27]. The surface-modifying microorganisms are known to produce phospholipid wetting agents or surfactants [28] which enable subsequent mechanical treatments to dissemble and separate otherwise tightly bound composite matrices.

The bacterium *Thiobacillus ferrooxidans* has been used in preoxidation treatments of gold and silver ores [29]. These precious metals often occur finely disseminated in iron pyrites which *T. ferrooxidans* oxidizes readily. Preoxidation of such ores improves gold and silver recoveries by subsequent conventional extraction methods.

2.1.2 Mineral Solubilization by Cells and Cell-Free Metabolites. Pyrite (FeS_2) oxidation by *T. ferrooxidans*, catalyzed by direct enzymatic attack and by biogenic acidic ferric sulfate solutions, is accelerated by a factor of up to 10^6 over the abiotic rate [30] with important industrial and environmental consequences. Microbially catalyzed pyrite oxidation is responsible for the production of acidic coal mine drainage. However, the acidic ferric sulfate solutions generated by this oxidation also solubilize metal sulfides in mining operations employing bioleaching.

Clear evidence was recently presented showing severe corrosion of structural iron artifacts by anaerobic bacterial production of as yet unidentified metabolites transmitted in solution or in respirant atmosphere [31].

Other evidence for a number of metabolic agents, themselves either of organic or inorganic nature, suggests that microbial solubilization of minerals is naturally widespread or can be exploited in chemical plant scale. Some of the key agents released by living cells may solubilize otherwise commonly highly refractory substances such as mineral ores, ceramics, and bulk metals as summarized in table 3. However, most of the reactions reported (table 3) have not identified the specific molecular entities produced by cells, nor quantitated the mechanistic path of solubilization. Recent preliminary work at NBS illustrates one mechanism of mineral sulfide solubilization by the pervasive algal metabolite methyl iodide. This metabolite appears to break metal-sulfur bridges by oxidative addition at sulfur or metal centers, weakening the crystal lattice and eventually allowing the metal to dissolve.

Production of powerful biogenic solubilizing agents can cause problems in process containment. Studies on corrosion resistance of materials to these metabolites are warranted.

2.1.3 Membrane and Cytoplasmic Uptake and Selective Precipitation of Elements. As ultratrace chemical speciation methods have gained favor and applicability, evidence has grown to support novel use of molecular topology arguments as structure-activity predictors for cell uptake of several metal species, notably tin [39]. Transmission of certain chemical forms of metals and metalloids across membranes occupies much attention of toxicologists and molecular geneticists [40] but much additional research is needed to complete our understanding of superficial membrane complexation of metal and metalloid ions, their entry into cell interiors and their ultimate fate. Nonetheless, progress has been made in describing bacterial uptake-transmission of isostructural, isoelectronic, and isosteric agents, as illustrated by the arsenate-phosphate [9], divalent cations [41], organotins [42] cases. Far more difficult will be the establishment of underlying biochemical factors that control the rate and extent of precipitation and morphology of those elements and their compounds that actually agglomerate in diffuse or specific sites within living cells. The case of *Aquaspirillum magnetotacticum*, a widely distributed aquatic bacterium, is of special interest because of its highly efficient and selective uptake of Fe(III) from solution, concentration, and derivatization to pure magnetite ultramicrocrystals aligned within the cell major axis [43]. The commercial consequences of understanding the mechanisms involved in such biosynthesis of hyperferromagnetic ultraparticles are significant especially in view of prospects for other strategic metals compounds.

2.2 Element-Specific Detection, Imaging, and Quantitation

From the foregoing discussion it is evident that progress is needed in defining tell-tale chemical reactions and their rate-determining participants within the controlling biological matrices. Understanding these processes requires measurements with a high degree of element- and species-specificity and extremely low detection limits characteristic of living cells. These general requirements for ultratrace analysis of chemical speciation of heavy elements undergoing con-

Table 3. Examples of metal solubilization by low-molecular weight extracellular metabolites.

Metabolite	Source Organism	Substrate	Product	Ref.
Methyl iodide	Marine algae	Metal sulfides	Soluble metal	32
		SnS	CH_3SnI_3	33
Siderophores	Bacteria	$Fe(OH)_3$	Iron chelates	34
Unidentified	Bacteria	Au	Soluble gold	38
Unidentified	SO_4^{2-} reducing bacteria	Fe^0, steel	Soluble Fe	31
		brass	Soluble Cu	31
Unidentified	*Penicillium*	Fe^0, steel	Soluble Fe	35
		Chalcocite ore	Soluble Cu	36
Methylcobalamin	Bacteria	Pb, Sn oxides	Soluble Pb,	37
			methyltin	37

trolling bio-transformations have received recent review [44], but several basic points merit emphasis in addition to common features of preconcentration, molecular separation, and selective detection within meaningful time frames. Chemical speciation of important bioprocess products may be required in solution, gas phase, on surfaces, or intracellularly.

2.2.1 Element Speciation in Cellular Media. Our laboratory has developed chromatographic systems (HPLC, GC) coupled with element-selective detectors for speciation of metal-containing biogenic molecules in gas or liquid phases at ultratrace (pg-ng) levels. Volatile forms of metals have been speciated by GC-AA [45,46], or by GC with a flame photometric detector made selective for the element of interest by different flame gas flows and optical interference filters [47]. Solvated forms of metals can be speciated using liquid chromatography coupled with atomic absorption [48] or epifluorescence microscope (using fluorescent ligands) [49,50] detectors.

2.2.2 Element Speciation at Substrate or Cell Surfaces. Methods for chemical speciation on surfaces are not as well developed as for liquid or gas media. It may be possible to dissolve or extract the material of interest from cells and perform analyses described above. We were able to measure the accumulation of tributyltin species on estuarine bacteria by HPLC-GFAA analyses of methanol extracts of cells [51]. More promising is the potential for using element- and chemical species-selective fluorescent ligands for imaging these molecules on cell or substrate surfaces. Recent work in our laboratories suggests that inorganic and organotin species accumulation on bacterial cells can be monitored using a fluorescent ligand, 3-hydroxyflavone with detection by epifluorescence microscopy [52] in which the microscope isequipped with a monochromator and photometer for measuring fluorescence emission intensities at appropriate wavelengths. Another surface analysis technique, Fourier transform infrared spectroscopy, is promising for study of biological reactions at surfaces. We have begun to apply FTIR to analyze biotransformation of coal leading to removal of specific undesirable functional groups [53]. Others are just beginning to study biofilms with this method [54].

2.2.3 Element Speciation Within Cells. Intracellular microbial processing products may be studied by breaking cells (sonication, pressure disruption, chemical treatments) and analyzing their contents by methods described above. Electron microscopy with x-ray microanalysis is useful for spatial characterization of elements in cells. However, nondestructive methods for speciation of process intermediates or products occurring intracellularly are more difficult. Nevertheless, recent progress in nuclear magnetic resonance spectroscopy has led to the application of this nondestructive technique to real-time monitoring of cellular metabolic processes [55].

Early work in the field of small angle neutron scattering (SANS) techniques for investigating protein structure is being undertaken [56]. However, the potential for studying intracellular metabolic processes has not been investigated. A particularly attractive model system for studying the application of SANS to biological transformations of materials is *Aquaspirillum magnetotacticum*—a magnetotactic bacterium that intracellularly deposits pure magnetite crystals on the order of 500 Å diameter [43]. We have undertaken preliminary experiments using SANS to measure magnetite particle formation rates in cells and to better understand how the cells can perform such an exact synthesis, in terms of size and purity, of these hyperferromagnetic particles.

2.3 Chemical Speciation and Process Monitoring

Materials bioprocessing will increasingly require monitoring of intermediates and products diagnostic of proper or optimal conditions. A better understanding of the enzymatic transformations of toxic metals by metal resistant process organisms is also needed. This includes analyzing metal speciation in solution and gas phases and bound to cell surfaces or precipitates. Many of the measurement techniques described in the previous sections may find application for such requirements. For example, the presence of toxic metals, such as Hg, in metal ore bioleaching systems has been suspected of inhibiting the beneficial action of the process organsims. Results in our laboratory and elsewhere showed that mercuric ions at concentrations as low as 10 μg/L inhibit iron oxidation by *Thiobacillus ferrooxidans* [57]. Iron is an energy source for the organism, and is added to the growth medium at 10–40 g/L levels. However, we have isolated a mercury-resistant strain of this organism and, using a gas chromatograph coupled with a flameless mercury atomic absorption detector, determined that the organism reduced Hg^{2+} to Hg° which was rapidly volatilized from the growth medium [57]. Thus, it is evident that mercury resistant strains of this species can be selected for by mercury in the environment. In collaboration with molecular biologists at Washington University, we characterized

the mechanism of reduction and found that the organism produces a heat-stable, intracellular mercuric reductase enzyme that uses reduced nicotinamide adenine dinucleotide phosphate (NADPH) as an electron donor [58]. With this information, a selectable genetic marker is now available for others to study in more detail, using recombinant DNA techniques, the genetics of this important industrial organism.

3. Current NBS Activities in Inorganic Materials Bioprocessing

Exciting new prospects for inorganic materials bioprocessing are presented by some of the recently discovered thermophilic bacteria (fig. 1). These include *Sulfolobus* [59] and other bacteria [60] discovered in hot springs and ore dumps, and the extreme thermophiles associated with volcanic activity in shallow [61] and deep [62] ocean depths where water exists in liquid form above 100 °C. These metal-enriched vent waters support novel microorganisms which potentially are applicable to metals bioprocessing since biological and chemical reactions are accelerated under increased temperature and pressure. We have recently begun a project to evaluate the bioleaching and recovery of strategic metals, in part using thermophilic microorganisms to accelerate reactions. In addition to high temperature (50–100 °C) studies at ambient pressures, a high pressure-temperature bioreactor will be employed to study metal bioprocess rates at pressures up to 250 atmospheres and temperatures of up to 200 °C.

Containment and process monitoring becomes difficult under the above conditions, especially when low pH and corrosive metabolites are involved. Conventional steels and plastics undergo deterioration under these extreme conditions [63] and alternative materials such as advanced ceramics will be required for any future industrial applications. The economics of metal processing under such conditions will be dictated by the value of the material and the enhancement or uniqueness of microbial processing compared to chemical or physical techniques.

The processing of metals using exocellular microbial metabolites is also under investigation. We found bulk metals and metal sulfides to be dissolved by methyl iodide (table 3), a common algal and fungal metabolite. Currently, we are examining processing of ores by MeI and other biogenic metabolites. It may be possible to generate such

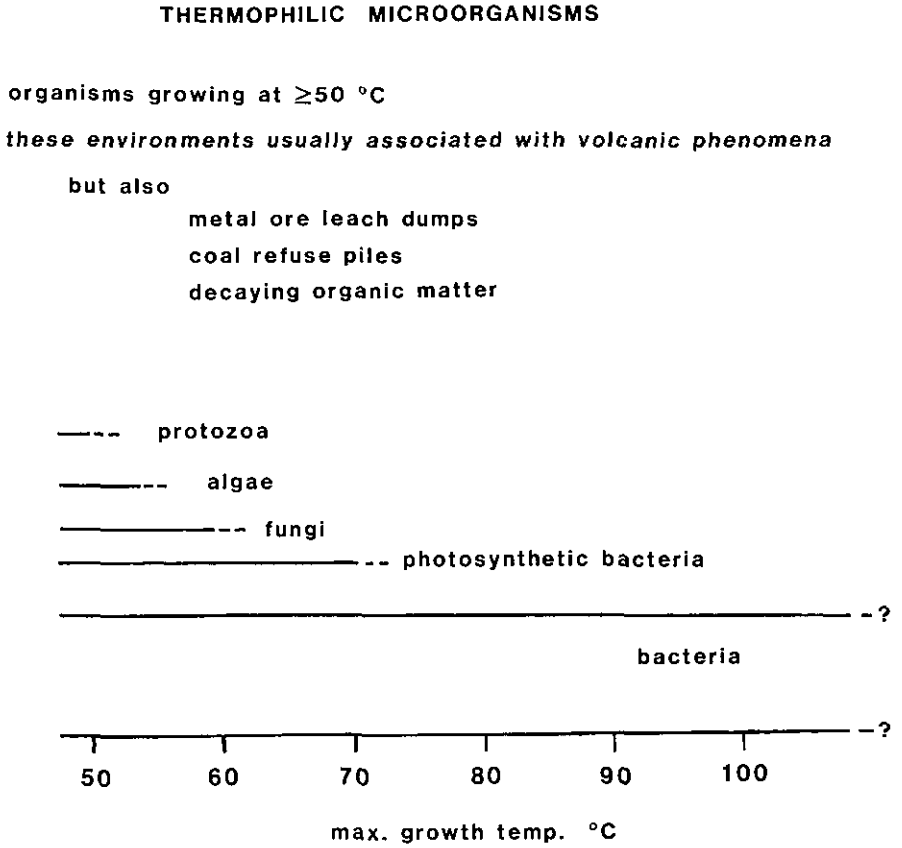

Figure 1–The relationship between maximum growth temperatures and various genera of microorganisms are compared, along with common environments supporting their growth. Newly discovered thermophilic bacteria have been shown to grow at 115 °C under pressure [61]. Unconfirmed reports of microbial growth at 250 °C and 200 atmospheres pressure have recently appeared [62].

metabolites in remote bioreactors and apply the solutions to the material to be processed.

We are also investigating prospects for using microorganisms for synthesis of selected metal forms. For example, certain thermophilic algae precipitate nickel as the sulfide exocellularly [26], magnetotactic bacteria produce magnetite crystals from soluble iron [43], and *Thiobacillus* and other resistant bacteria reduce mercuric ions to elemental mercury. The use of such organisms to produce desired molecular forms of strategic or precious metals is under investigation in our laboratories.

4. Conclusions

Man has used biotechnology for centuries, initially for fermentations and more recently in the food, pharamaceutical, and medical fields. However, we are only beginning to understand how to apply microorganisms for the recovery and processing of inorganic materials for commercial and technological applications. Our knowledge is incomplete in understanding mechanisms of microbial interactions with inorganic or heavy elements which may be transformed as energy sources, electron acceptors in respiration, or as toxic agents. Chemical speciation of such elements in aqueous, gaseous, or cellular media is essential in understanding mechanisms of biotransformations. Surface analysis or imaging is important because many biotransformations of these heavy elements involve reactions of insoluble substrates or precipitation. Newly discovered microorganisms in metal-rich thermal environments offer exciting prospects for novel and accelerated bioprocessing.

In summary, a materials cycle is presented (fig. 2) which illustrates the potential microbial role in

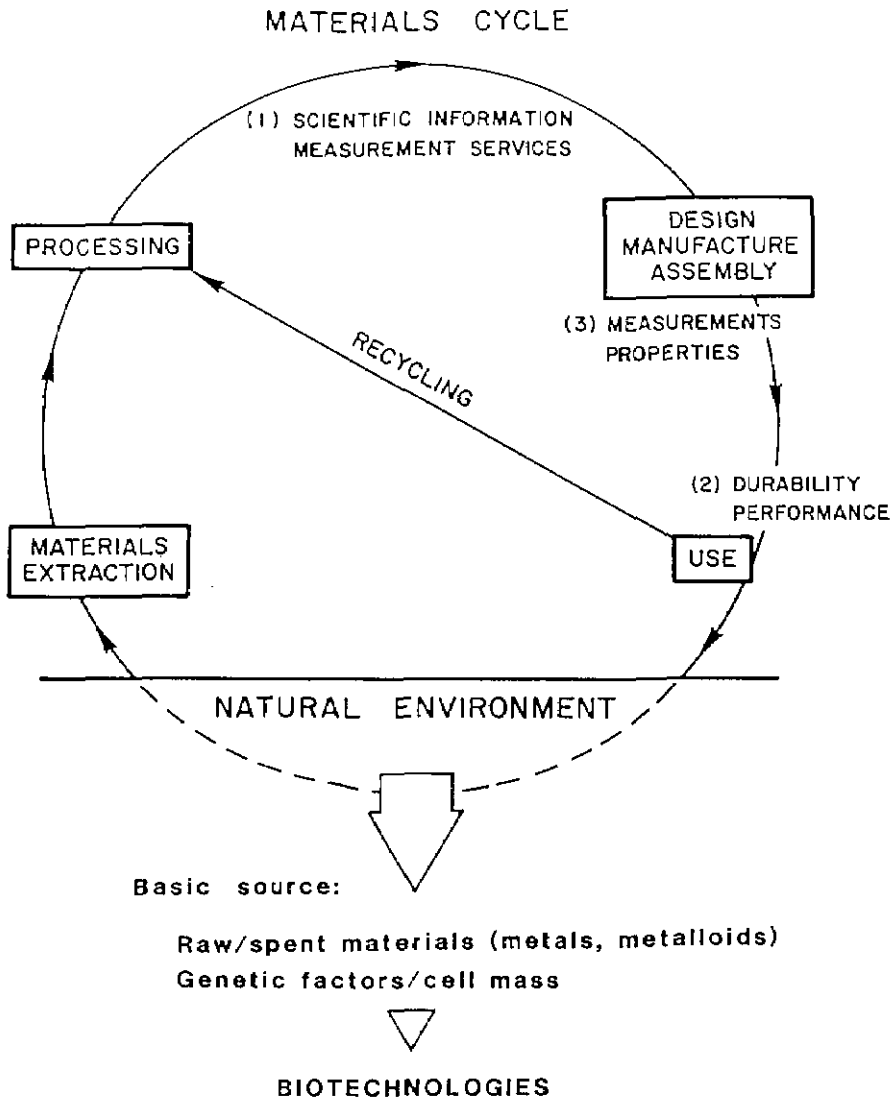

Figure 2-The conventional "cross-cutting" features of measurements in relation to materials design, processing, use and recycling are here defined in terms of their frequent natural environmental interactions. Thereby, a coherent picture of new materials innovation and acquisition emerges in terms of biotechnological options.

acquisition and disposition of materials (the lower portion of the circle). We have shown the importance of and potential for microorganisms in materials extraction and for recovering and recycling of heavy elements from waste or process streams. Also, future developments in processing elements into selected forms appears promising.

References

[1] Anonymous. What is biotechnology? Anal. Chem. **56**, 1550A (1984).

[2] Campbell, M. C., Canadian government activities in biotechnology as it applies to the mineral industry. Paper presented at workshop for the Mining, Metal-Refining and Fossil Fuel Processing Industries, Troy, NY (May 28–30, 1985).

[3] Bowers, E. W., Steel in search of leapfrog technology, Iron Age **227**, 60–63 (1984).

[4] Ehrlich, H. L., Geomicrobiology, New York: Marcel Dekker (1981).

[5] Baross, J. A.; M. D. Lilley and L. I. Gordon, Is the CH_4, H_2, and CO venting from submarine hydrothermal vent systems produced by thermophilic bacteria? Nature **298**, 366–368 (1982).

[6] D'Itri, F. M., The environmental mercury problem, Cleveland: CRC Press (1972)

[7] Silver, S., Bacterial transformations of and resistances to heavy metals, in Changing Biogeochemical Cycles of Metals and Human Health, Berlin: Springer-Verlag (in press).

[8] Summers, A. O., Genetic adaptations involving heavy metals. In Current Perspectives in Microbial Ecology, M. J. Klug and C. A. Reddy, eds., Washington: American Society for Microbiology, 94–104 (1984).

[9] Silver, S., and D. Keach, Energy-dependent arsenate efflux: The mechanism of plasmid mediated resistance, Proc. Natl. Acad. Sci. USA **79**, 6114–6118 (1982).

[10] McHugh, G. L.; R. C. Moellering, C. C. Hopkins, and M. N. Swartz, *Salmonella typhimurium* resistant to silver nitrate, chloramphenicol, and ampicillin. Lancet i: 235–239 (1975).

[11] Tynecka, Z.; Z. Gos and J. Zajac, Energy-dependent efflux of cadmium coded by a plasmid resistance determinant in *Staphylococcus aureus*. J. Bacteriol. **147**, 313–319 (1981).

[12] Williams, J. W., and S. Silver, Bacterial resistance and detoxification of heavy metals. Enzyme Microb. Technol. **6**, 530–537 (1984).

[13] Ingledew, J., *Thiobacillus ferrooxidans:* The bioenergetics of an acidophilic chemolithotroph, Biochim. Biophys. Acta **683**: 89-117 (1982).

[14] Lyalikova, N. N., Oxidation of trivalent antimony up to higher oxides as a source of energy for the a new autotropic organism, Stibiobacter, gen. nov. Dokl. Akad. Nauk SSSR **205**, 1228–1229 (1972).

[15] DiSpirto, A. A., and O. H. Tuovinen, Uranous ion oxidation and carbon dioxide fixation by *Thiobacillus ferrooxidans,* Arch. Microbiol. **133**, 28–32 (1982).

[16] Nielsen, A. M., and J. V. Beck, Chalcocite oxidation and coupled carbon dioxide fixation by *Thiobacillus ferrooxidans*. Science **175**, 1124–1126 (1972).

[17] Zajic, J. E., Microbial biogeochemistry, New York: Academic Press, 170–171 (1969).

[18] Ehrlich, H. L., Inorganic energy sources for chemolithotrophic and mixotrophic bacteria, Geomicrobiol. J. **1**, 65–83 (1978).

[19] Brinckman, F. E.; G. J. Olson and W. P. Iverson, The production and fate of volatile molecular species in the environment: metals and metalloids. In Atmospheric Chemistry, E. D. Goldberg, ed., Berlin: Springer-Verlag 231–249 (1982).

[20] Brierley, C. L., Bacterial leaching. CRC Crit. Rev. Microbiol. **6**, 207–262 (1978).

[21] MacGregor, R. A., Uranium dividends from bacterial leaching. Mining Engin. 54–55 (1969 March).

[22] Sterritt, R. M., and J. N. Lester, The microbiological control of mine waste pollution. Miner. Environ. **1**, 45–47 (1979).

[23] Strandberg, G. W.; S. E. Shumate and J. R. Parrott, Microbial cells as biosorbents for heavy metals: Accumulation of uranium by *Saccharomyces cerevisiae* and *Pseudomonas aeruginosa*. Appl. Environ. Microbiol. **41**, 237–245 (1981).

[24] Belly, R. T., and G. C. Kydd, Silver resistance in microorganisms. Dev. Ind. Microbiol. **23**, 567–577 (1982).

[25] Bruynesteyn, A., Biological and chemical processing of low grade ores, in Chemistry for the Future, H. Grunewald, ed., Oxford: Pergamon Press, 301–304 (1983).

[26] Wood, J. M., and H. K. Wang, Microbial resistance to heavy metals. Environ. Sci. Technol. **17**, 582A–590A (1983).

[27] Kempton, A. G.; N. Moneib, R. G. L. McCready, and C. E. Capes, Removal of pyrite from coal by conditioning with *Thiobacillus ferrooxidans* followed by oil agglomeration. Hydrometallurgy **5**, 117–125 (1980).

[28] Schaeffer, W. I., and W. W. Umbreit, Phosphotidylinositol as a wetting agent in sulfur oxidation by *Thiobacillus thiooxidans*. J. Bacteriol. **85**, 492–493 (1962).

[29] Lawrence, R. W., and A. Brunsteyn, Biological pre-oxidation to enhance gold and silver recovery from refractory pyritic ores and concentrates. CIM Bull. **76**, 107–110 (1983).

[30] Singer, P. C., and W. Stumm, Acidic mine drainage: The rate-determining step, Science **167**, 1121–1123 (1970).

[31] Iverson, W. P., An overview of the anaerobic corrosion of underground metallic structures—evidence for a new mechanism, in Underground Corrosion, E. Escalante, ed., Philadelphia, PA: American Society for Testing and Materials, 33–52 (1981).

[32] Thayer, J. S.; G. J. Olson and F. E. Brinckman, Iodomethane as a potential metal mobilizing agent in nature, Environ. Sci. Technol. **18**, 726–729 (1984).

[33] Manders, W. R.; G. J. Olson, F. E. Brinckman, and J. M. Bellama, A novel synthesis of methyltin triiodide with environmental implications, J. Chem. Soc. Chem. Commun. 1984: 538–540 (1984).

[34] Raymond, K. N., and C. J. Carrano, Coordination chemistry and microbial iron transport, Acc. Chem. Res. **12**, 183–190 (1979).

[35] Siegel, S. M.; B. Z. Siegel and K. E. Clark, Bio-corrosion: Solubilization and accumulation of metals by fungi. Water, Air, Soil Pollut. **19**, 229–236 (1983).

[36] Wenberg, G. M.; F. H. Erbisch and M. E.Volin, Leaching of copper by fungi, Soc. Mining Engin., AIME **250**, 207–212 (1971).

[37] Thayer, J. S., and F. E. Brinckman, The biological methylation of metals and metalloids, in Organometallic

Chemistry, Vol. 20. F. G. A. Stone and R. West, eds., New York, NY: Academic Press, 313–356 (1982).

[38] LeRoux, N. W., Mineral attack by microbiological processes, in Microbial Aspects of Metallurgy, J. D. A. Miller, ed., New York, NY: American Elsevier, 173–182 (1970).

[39] Laughlin, R. B.; R. B. Johannesen, W. French, H. E. Guard, and F. E. Brinckman, Structure-activity relationships for organotin compounds. Environ. Toxicol. Chem. **4**, 343–351 (1985).

[40] Silver, S., Mechanisms of bacterial resistances to toxic heavy metals: arsenic, antimony, silver, cadmium, and mercury, in Environmental Speciation and Monitoring Needs for Trace Metal-containing Substances From Energy-related Processes. F. E. Brinckman and R. H. Fish, eds., National Bureau of Standards, Spec. Publ. 618 (1981).

[41] Silver, S., Magnesium transport in microorganisms, in Microorganisms and Minerals, E. D. Weinberg, ed., New York: Marcel Dekker, 7–47 (1977).

[42] Wong, P. T. S.; Y. K. Chau, O. Kramar, and G. A. Bengert, Structure-toxicity relationships of tin compounds on algae, Can. J. Fish. **39**, 483–488 (1982).

[43] Blakemore, R. P., Magnetotactic bacteria. Ann. Rev. Microbiol. **36**, 217–238 (1982).

[44] Thayer, J. S., and F. E. Brinckman, The biological methylation of metals and metalloids, in Advances in Organometallic Chemistry, F. G. A. Stone and R. West, eds., New York: Academic Press, 313–356 (1982).

[45] Blair, W.; W. P. Iverson and F. E. Brinckman, Application of a gas chromatograph-atomic absorption detection system to a survey of mercury transformations by Chesapeake Bay microorganisms. Chemosphere **3**, 167–174 (1974).

[46] Parris, G. E.; W. R. Blair and F. E. Brinckman, Chemical and physical considerations in the use of atomic absorption detectors coupled with a gas chromatograph for determination of trace organometallic gases, Anal. Chem. **49**, 378–386 (1977).

[47] Jackson, J. A.; W. R. Blair, F. E. Brinckman, and W. P. Iverson, Gas chromatographic speciation of methylstannanes in the Chesapeake Bay using purge and trap sampling with a tin-selective detector, Environ. Sci. Technol. **16**, 110–119 (1982).

[48] Parks, E. J.; F. E. Brinckman and W. R. Blair, Application of a graphite furnace atomic absorption detector automatically coupled to a high-performance liquid chromatograph for speciation of metal-containing macromolecules, J. Chromatogr. **185**, 563–572 (1979).

[49] Parks, E. J.; W. R. Blair, G. J. Olson, F. E. Brinckman, and M. C. Valeris-Price, manuscript in preparation.

[50] Parks, E. J.; W. R. Blair, G. J. Olson, F. E. Brinckman, and M. C. Valerias-Price, and J. C. Means, Ultratrace speciation of organometallic species in natural systems, using microbore and capillary techniques with an epifluorescence microscope imaging detector. Pittsburgh Conf. Anal. Chem., New Orleans, LA (March 1985).

[51] Blair, W. R.; G. J. Olson, W. P. Iverson, and F. E. Brinckman, Accumulation and fate of tri-n-butyltin cation in estuarine bacteria. Microb. Ecol. **8**, 241–251 (1982).

[52] Brinckman, F. E., and G. J. Olson, Chemical principles underlying bioleaching of metals from ores and solid wastes and bioaccumulation of metals from solutions. Biotechnol. Bioengin. Symp. (in press).

[53] Olson, G. J.; F. E. Brinckman and W. P. Iverson, Bioprocessing coal with microorganisms. Proceedings report for Electric Power Research Institute (April 1985).

[54] Nichols, P. D.; J. M. Henson, J. B. Guckert, D. E. Nivens, and D. C. White, Fourier transform-infrared spectroscopic methods for microbial ecology; analysis of bacteria, bacteria-polymer mixtures and biofilms. J. Microbiol. Methods **4**, 79–94 (1985).

[55] Scott, A. I., and R. L. Baxter, Applications of ^{13}C NMR to metabolic studies. Ann. Rev. Biophys. Bioeng. **10**, 151–174 (1981).

[56] Stuhrmann, H. B., and A. Miller, Small angle scattering of biological structures. J. Appl. Cryst. **11**, 325–345 (1978).

[57] Olson, G. J.; W. P. Iverson and F. E. Brinckman, Volatilization of mercury by *Thiobacillus ferrooxidans*, Curr. Microbiol. **5**, 115–118 (1981).

[58] Olson, G. J.; F. D. Porter, J. Rubinstein, and S. Silver, Mercuric reductase enzyme from a mercury-volatilizing strain of *Thiobacillus ferrooxidans*, J. Bacteriol. **151**, 1230–1236 (1982).

[59] Brock, T. D.; K. M. Brock, R. T. Belly, and R. L. Weiss, Sulfolobus: A new genus of sulfur-oxidizing bacteria living at low pH and high temperature. Arch. Microbiol. **84**, 54–68 (1972).

[60] Norris, P. R.; J. A. Brierley and D. P. Kelly, Physiological characteristics of two facultatively thermophilic mineral-oxidizing bacteria. FEMS Microbiol. Lett. **7**, 119–122 (1980).

[61] Stetter, K. O.; H. Konig and E. Stackebrandt, *Pyrodictium*: gen. nov., a new genus of submarine disc-shaped sulfur reducing archaebacteria growing optimally at 105 °C, System. Appl. Microbiol. **4**, 535–542 (1983).

[62] Baross, J. A., and J. W. Deming, Growth of "black smoker" bacteria at temperatures of at least 250 °C, Nature **303**, 423–426 (1983).

[63] Sonnleitner, B.; S. Cometta and A. Fiechter, Equipment and growth inhibition of thermophilic bacteria, Biotechnol. Bioengin. **24**, 2597–2599 (1982).

Journal of Research of the National Bureau of Standards

Improvements in the Application Of the Numerical Method of Characteristics To Predict Attenuation in Unsteady Partially Filled Pipe Flow

Volume 91 Number 3 May–June 1986

John A. Swaffield and Katrina Maxwell-Standing

Brunel University, Uxbridge, Middlesex, United Kingdom

The use of linear interpolation and simplified iteration procedures are shown to introduce inaccuracies to the rectangular grid method of characteristics, particularly when applied to subcritical flows. Comparisons of experimental and computational results are presented illustrating the use of Everett and Newton-Gregory interpolation, in addition to a more complex iteration procedure, to substantially improve the method's ability to maintain both steady uniform flows under subcritical conditions, and retain wave steepness during propagation along the drainage pipe. The results presented will be directly applicable to the building drainage network model previously developed at Brunel University with the support of NBS CBT grant aid.

Key words: integration; interpolation; method of characteristics; rectangular grid (R.G.).

Accepted: February 25, 1986

1. Introduction

A computer model that will simulate the propagation of steep fronted waves along a drainage pipe is being developed from recent research by Bridge [1][1] and Swaffield et al. [2]. The rectangular grid (R.G.) method of characteristics, employed to solve numerically the appropriate unsteady flow equations, was used to model the attenuation of the flow profiles in the pipe. Several papers describe the derivation and applications of the numerical solutions of the governing equations for transient partially filled pipe flow [1,2,3]. This paper presents results of an investigation into the computational problems identified by Swaffield and Bridge. One example is the collapse of the water surface profile over time during the passage of steady flows under subcritical conditions. It was felt that these inaccuracies were probably caused by the linear interpolation and simplified iteration procedures being used within the method of characteristics.

Numerous computer runs were made to determine if the accuracy of the method could be improved by employing a nonlinear interpolation procedure and by using a more complex iteration procedure. The computed results were compared to data from experiments carried out on the Brunel test rig.

About the Authors: John A. Swaffield was with Brunel when the work described was performed. He is now a professor in the Department of Building, Heriot-Watt University, Edinburgh, Scotland. Katrina Maxwell-Standing is with Brunel's Mechanical Engineering Department. The research was conducted under NBS Grant No. 60NANB5D0510.

[1] Figures in brackets indicate literature references.

NOTATION

A = water depth cross-sectional area (m^2)

c = local wavespeed (m/s)

D = pipe diameter (m)

f_n = $f(x_n)$

g = acceleration due to gravity (m/s^2)

h = constant step length (m)

S_0 = pipe slope

S_f = slope of energy grade line

T = water surface width (m)

t = time (s)

$TFAC$ = time factor

V = local flow average velocity (m/s)

x = distance from upstream boundary (m)

y = local flow depth (m)

$\delta^i f_n$ = i^{th} central difference at $x = x_n$.

2. The Rectangular Grid Method of Characteristics

The St. Venant equations are a pair of quasi-linear hyperbolic partial differential equations. The equation of continuity is expressed

$$V\frac{\partial A}{\partial x}+A\frac{\partial V}{\partial x}+T\frac{\partial y}{\partial t}=0 \tag{1}$$

and the dynamic equation,

$$g\,(S_f-S_0)+g\frac{\partial y}{\partial x}+V\frac{\partial V}{\partial x}+\frac{\partial V}{\partial t}=0. \tag{2}$$

The St. Venant equations can be transformed into their characteristics in a number of ways; Fox [3] gives one method. The equations describing the positive and negative characteristics are:

$$\frac{dV}{dt}+\frac{g}{c}\frac{dy}{ct}+g\,(S_f-S_0)=0 \tag{3}$$

$$\frac{dx}{dt}=V+c \tag{4}$$

$$\frac{dV}{dt}-\frac{g}{c}\frac{dy}{dt}+g\,(S_f-S_0)=0 \tag{5}$$

$$\frac{dx}{dt}=V-c \tag{6}$$

where $c=g\sqrt{A/T}$. The positive characteristic is described by eqs (3 and 4) and the negative characteristic by (5 and 6).

These equations are then numerically integrated. An approximation is introduced in the integration of some terms as the variation of V and y is not known as a function of time. Referring to figure 1, if the velocity and depth are known at points R and S at time level $t-\Delta t$ then a first-order approximation leads to the following set of equations which may be written in terms of the unknown depth and velocity at point P at time level t,

$$V_P-V_R+\frac{g}{c_R}(y_P-y_R)+g\,(S_R-S_0)\,\Delta t=0 \tag{7}$$

$$x_P-x_R=(V_R+c_R)\,\Delta t \tag{8}$$

$$V_P-V_S+\frac{g}{c_s}(y_P-y_S)+g\,(S_S-S_0)\,\Delta t=0 \tag{9}$$

$$x_P-x_S=(V_S-c_S)\,\Delta t\,. \tag{10}$$

These equations are paired such that eq (7) is true only if eq (8) is satisfied and similarly for eqs (9 and 10). In most cases a first order integration is satisfactory, however attention must be given to the choice of the time step to ensure a stable solution, as mentioned in [3]. Generally, applying the Courant condition,

$$\Delta t=\frac{\Delta x}{(V+c)_{max}} \tag{11}$$

ensures that the points R and S fall within $\pm\,\Delta x$ of point P. Since the velocity and celerity both vary throughout the duration of the analysis the maximum value of each is found at every time step.

The algebraic solution of eqs (7–10) reduces to a problem of determining the values of x_R, y_R, V_R, x_S, y_S and V_S since x_p, t_p, t_R and t_S are known values. Referring to figure 1, x_R and x_S are determined by using eqs (4 and 6) respectively to estimate the t-Δt line intersections of the positive and negative characteristtics passing through point P. The quantities y_R, y_S, V_R and V_S are then determined by interpolation between grid points A and C and C and B respectively for this example of subcritical flow.

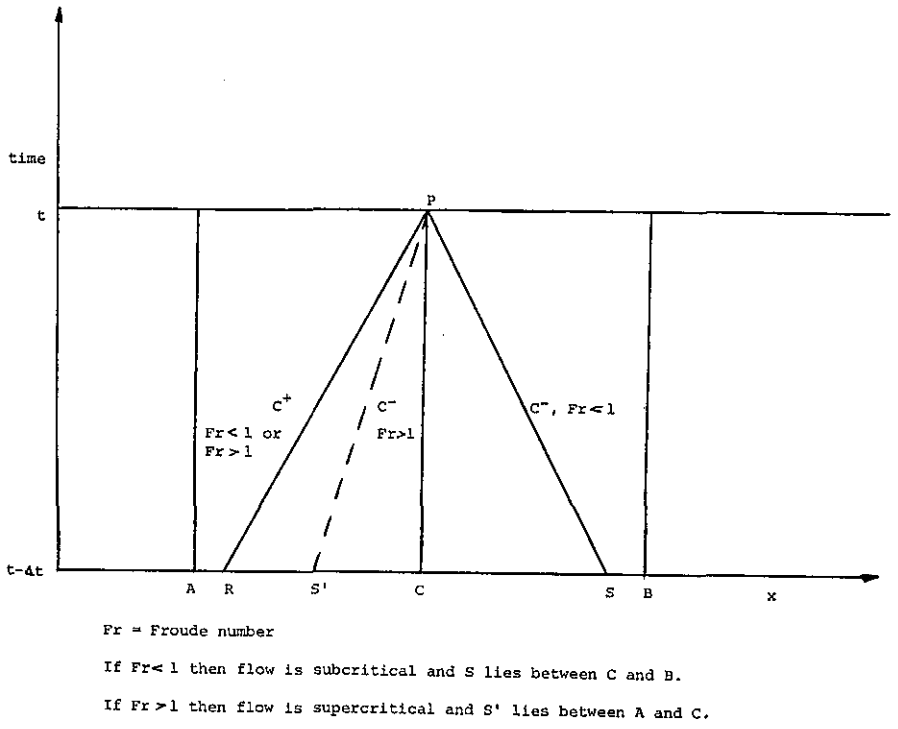

Figure 1–Specified time interval technique.

Finally the solution to point P is obtained through the simultaneous solution of eqs (7 through 10).

3. Inaccuracies in the Method of Characteristics

A summary of the initial and boundary conditions required to apply the R.G. method of characteristics to drainage flow is presented in [1]. The method described above was used in a model simulating the movement of a hydraulic jump in a drainage pipe. Like Streeter and Wylie [4], the positions of x_R and x_s were determined by assuming that the slope of the characteristic lines at P were equal to those at C. The depth and velocity at points R and S were determined by linearly interpolating between grid points A and C and C and B (subcritical flow). However, it was found that two problems arose. The first being that the water surface profile downstream of the jump collapsed over time, and the second that the hydraulic jump acquired a positive velocity during the passage of steady flows. Harris [5] mentions that the Streeter-Wylie approximations are reasonable provided that the values of y and V at A, B and C do not differ greatly. The values of depth and velocity across a hydraulic jump or a steep-fronted wave do differ greatly; therefore, these approximations are not valid for the case being considered and a more exact method must be employed.

4. Improvement of the R.G. Method of Characteristics

4.1 Integration

There are several ways by which the R.G. method of characteristics can be made more accurate. One method [6] is to apply the trapezoidal rule when integrating the characteristic equations. However, the resulting equations must be solved by an implicit method. The implicit scheme is fairly complicated for open channel flow problems and is seldom used as it requires an iteration procedure. In addition, the benefits derived from the more accurate integration of the characteristic equations are often lost in the interpolation methods required to evaluate conditions at R and S.

4.2 Iteration

Accuracy can also be increased by using an iterative method to determine the positions of x_R and x_S from the slopes of the characteristics. A simplified iterative method similar to one developed by Lister [7] has been used to improve the computer model. The position of x_R is initially determined by assuming that the slope of the characteristic line at P is equal to that at C; y_R and V_R are then found from a nonlinear interpolation of values at surrounding gridpoints. (The exact interpolation method will be discussed below.) x_R is then recalculated assuming

that the slope of the characteristic line from P to R is equal to that of the previous value of x_R:

$$x_P - x_R^{(k+1)} = (V_R^k + c_R^k)\,dt\ . \tag{12}$$

This process is repeated until the difference between successive iterations of x_R is less than 0.001 meters. The same process is used to find x_S.

4.3 Interpolation

The inaccuracies caused by the effect of linearly interpolating between grid points to find the values of the depth and velocity at points R and S at each time step are illustrated in figure 2. The figure shows a section of backwater profile at the end of a pipe in which the flow is subcritical. Alternatively, this can be considered as the backwater profile between a hydraulic jump and a junction. For steady uniform flow the backwater profile should remain constant. However, linear interpolation between points A and C and points B and C produce values for depth at points R and S which are lower than the actual values. This leads to an underestimation of the depth at P at the next time step, which in turn leads to an overestimation of the velocity at P. These interpolation errors build up as the calculations continue in time causing the backwater profile to collapse and the discharge to increase. These effects have also been noted by Fox (see [1]).

Quadratic interpolation [7–9] and Langrangian [10–12] interpolation procedures have been used in the past to increase the accuracy of the R.G. method of characteristics. Jolly and Vevjevich [10] found that the Langrangian interpolation yielded more accurate results than linear interpolation. It was found that accuracy was not improved by using a more sophisticated scheme than third-order Langrangian interpolation equations combined with an iterative procedure to find the positions of R and S.

Although the Langrange method minimizes the amount of calculations it has the disadvantage that it gives no indication of the accuracy available. As a result, difference methods tend to be used in exploratory work and the Langrange methods in well-understood routine work [13]. In general, the error in using a difference method is of the order of the first term to be omitted. Formulae which involve central differences give the best accuracy for a given amount of computation. They also have the philosophical merit of giving equal weight to the tabulated data on each side of the relevant data point. The practical interpolation formulae are those of Everett and Bessel. If third differences are negligible for the accuracy required, then Bessel's formula is simpler and hence better. If third differences are greater than 60 units in the last decimal they cannot be neglected. Thus Everett's formula is best for our purposes [14]. Everett's formula involves only even-order central differences:

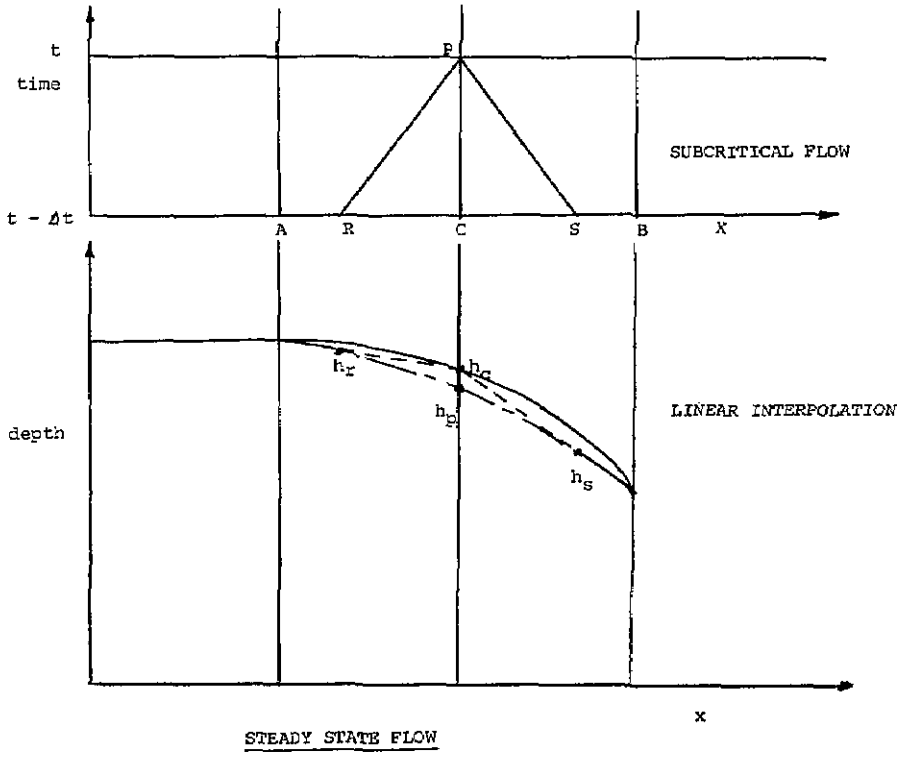

Figure 2–Interpolation error on the backwater profile.

$$P(x)=E_0 f_0+E_2\delta^2 f_0+E_4\delta^4 f_0+\ldots$$
$$+F_0 f_1+F_2\delta^2 f_1+F_4\delta^4 f_1+\ldots \quad (13)$$

where

$$E_0=1-u \quad (14)$$

$$E_2=\frac{-u(1-u)(2-u)}{3!} \quad (15)$$

$$E_4=\frac{-(-1-u)(u)(1-u)(2-u)(3-u)}{5!} \quad (16)$$

$$F_0=u \quad (17)$$

$$F_2=\frac{u(u^2-1)}{3!} \quad (18)$$

$$F_4=\frac{u(u^2-1)(u^2-4)}{5!} \quad (19)$$

and

$$u=\frac{(x-x_0)}{h}, \quad 0<u<1. \quad (20)$$

Near the ends of the pipe where central differences cannot be obtained the Newton-Gregory forward backward difference formulae are used. The Newton-Gregory forward difference formula is expressed by:

$$P(x)=P(x_0+hu)=f_0+u\Delta f_0+\frac{1}{2}\left[u(u-1)\Delta^2 f_0\right]$$
$$+\frac{1}{3!}\left[u(u-1)(u-2)\Delta^3 f_0\right]+\ldots$$
$$\ldots+\frac{1}{n!}\left[u(u-1)\ldots(u-n+1)\Delta^n f_0.\right] \quad (21)$$

and the backward difference formula by:

$$P(x)=P(x_0+hu)=f_0+u\nabla f_0+\frac{1}{2}\left[u(u+1)\nabla^2 f_0\right]$$
$$+\frac{1}{3!}\left[u(u+1)(u+2)\nabla^3 f_0\right]+\ldots$$
$$\ldots+\frac{1}{n!}\left[u(u+1)\ldots(u+n-1)\nabla^n f_0\right]. \quad (22)$$

5. Comparison of the Results

An example of the effects of linear interpolation can be seen in figure 3 which shows subcritical partially filled flow with a wave entering the pipe at a time of 0.23 seconds. As time progressed the backwater profile collapsed. A time factor, *TFAC*, of 5.0 was used in this example. The use of a time factor causes the time step eq (11) to become smaller:

$$\Delta t=\frac{\Delta x}{(V_{max}+c_{max})\,TFAC}. \quad (23)$$

It is important to determine a value of *TFAC* that results in a converged solution, whilst not requiring excessive computation time. If *TFAC* is chosen sufficiently large then a converged solution will always be achieved, provided that the results are not dominated by rounding and truncation errors. Generally, the smallest *TFAC* that will allow stability is

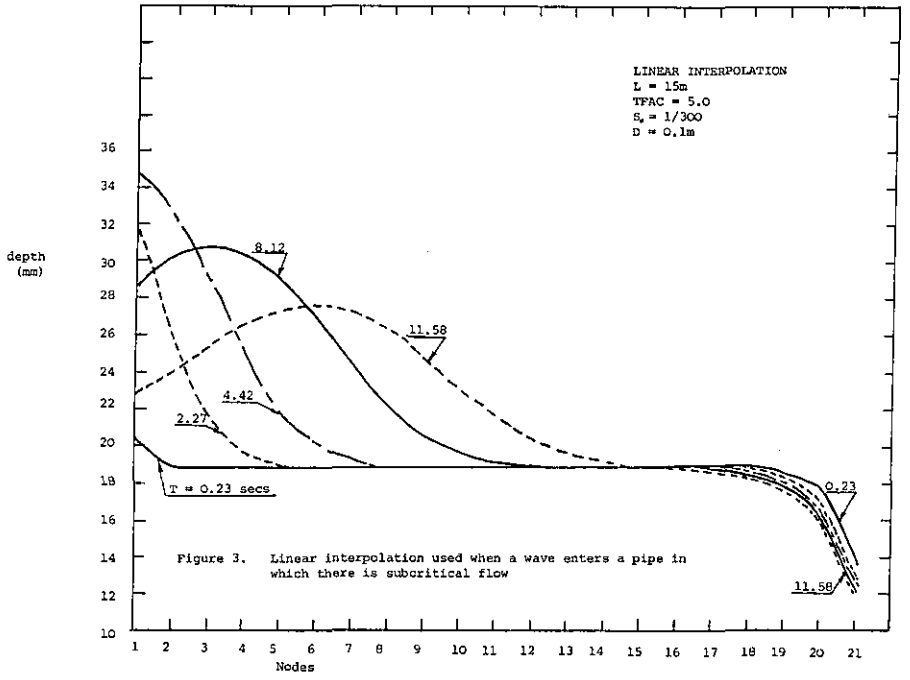

Figure 3–Linear interpolation used when a wave enters a pipe in which there is subcritical flow.

used. The time factors used in these results were determined by trial and error.

Figure 4 shows the effects of using Everett and Newton-Gregory interpolation on the same flow conditions of the previous example. A *TFAC* of 1.0 is the smallest *TFAC* that would allow stability, from eq (11). It can be seen that the backwater profile remained unchanged with increasing time. On comparing the two figures it can be seen that the linear method tended to flatten out the wave whereas Everett's method retained the wave's steepness. Everett's method also remained stable with a *TFAC* of 1.0. When linear interpolation was used with a *TFAC* of 1.0 a discontinuity developed on the wave front at a time of 11.31 seconds as shown in figure 5.

Figure 6 shows the experimentally measured depth profile at a distance of 8.0 meters from the entrance of the pipe against time. It can be seen that in this case both Everett's method and the linear interpolation method used with a *TFAC* of 1.0 retained the wave's steepness and compare most

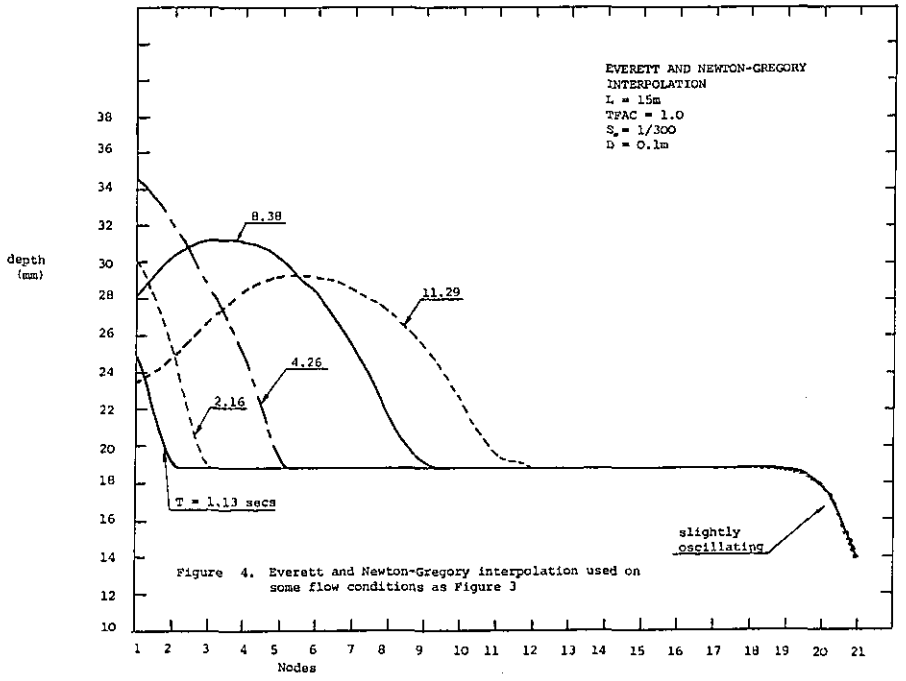

Figure 4. Everett and Newton-Gregory interpolation used on some flow conditions as Figure 3

Figure 4–Everett and Newton-Gregory interpolation used on some flow conditions as figure 3.

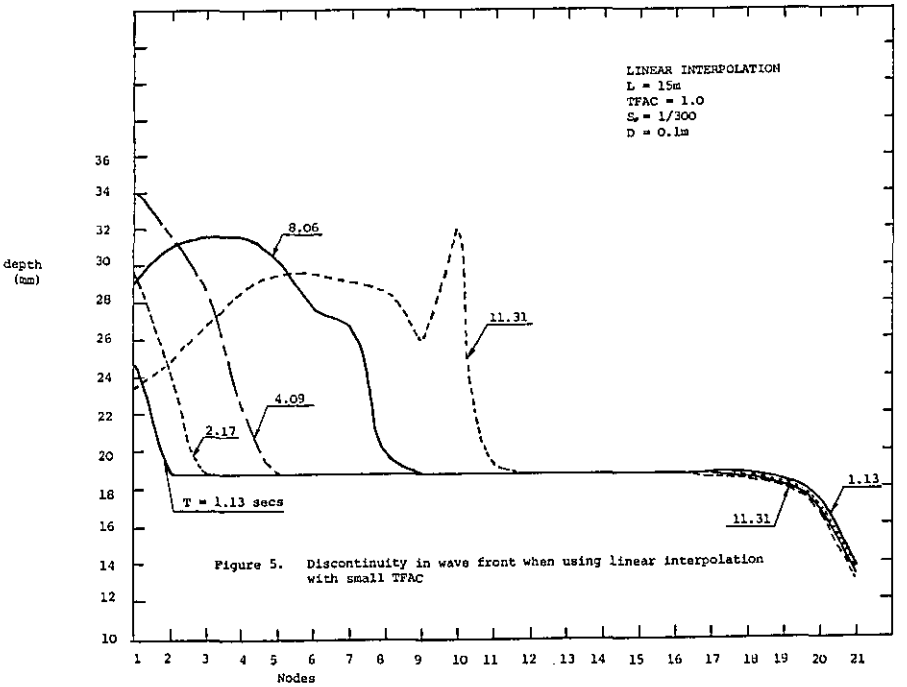

Figure 5. Discontinuity in wave front when using linear interpolation with small TFAC

Figure 5–Discontinuity in wave front when using linear interpolation with small *TFAC*.

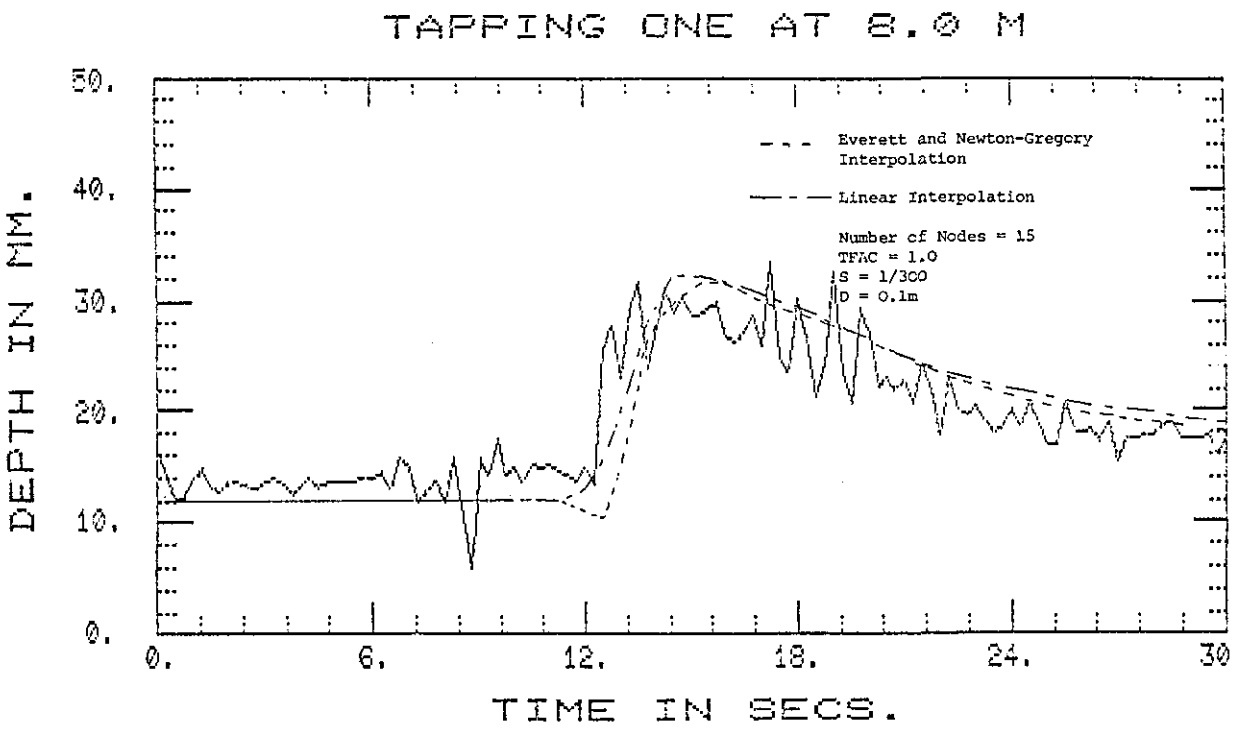

Figure 6–Comparison of experimental and computed results used to predict wave attenuation.

favorably with the experimental data from the Brunel test rig.

An increasing backwater profile is created where a drainage pipe joins a junction. Figure 7 shows the propagation of a wave entering such a pipe in a case where Everett and Newton-Gregory interpolation with a *TFAC* of 3.0 was used. It can be seen that the backwater profile remained steady and the steepness of the wave was retained. When linear interpolation was used with the same *TFAC* the backwater profile increased as time progressed. Thus Everett's method is clearly an improvement

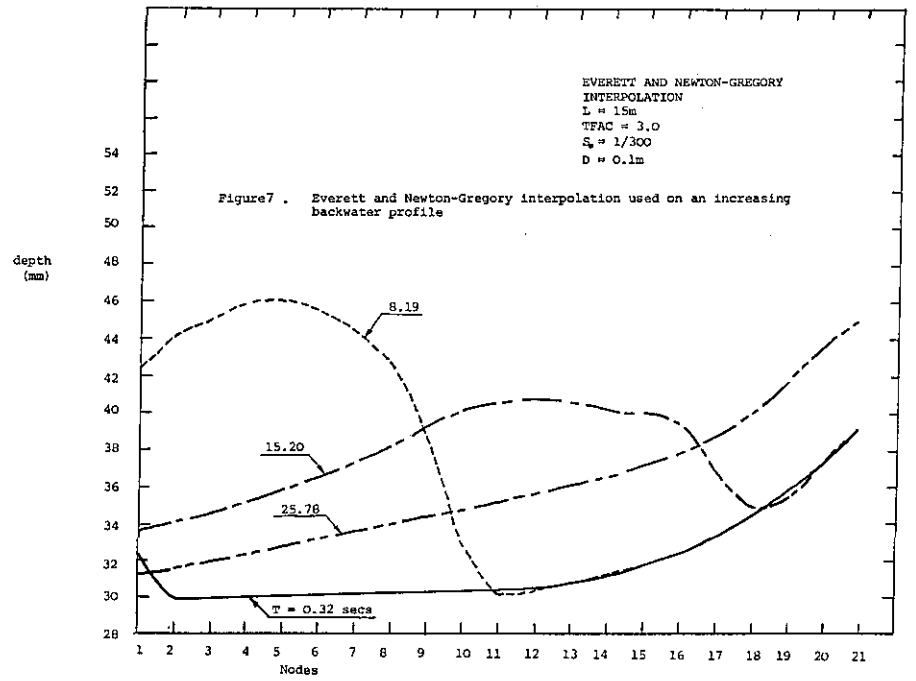

Figure 7–Everett and Newton-Gregory interpolation used on an increasing backwater profile.

to linear interpolation as it retains the backwater profile and wave steepness when run with a small *TFAC*.

6. Conclusions

A computer model, based on the rectangular grid method of characteristics that will simulate the propagation of steep fronted waves along a drainage pipe is being developed from recent research by Bridge and Swaffield [1,2]. Experimental tests carried out on the Brunel test rig as well as numerous computer runs have shown that the accuracy of the model has been considerably improved by including an interation procedure to find the positions of the space time coordinates R and S and also by using Everett's interpolation to determine the height and velocity at points R and S. The improvements made have solved the problem of the decreasing backwater profile during steady uniform flow noted by Bridge. The improvements also retain the steepness of waves shown in test data as they travel along the branch pipe.

References

[1] Bridge, S., A study of unsteady flow wave attenuation in partially filled pipe networks. Unpublished PhD thesis, Brunel University, May 1984.

[2] Swaffield, J. A.; S. Bridge and L. S. Galowin, Mathematical modelling of time dependent wave attenuation and discrete solid body transport in gravity driven partially filled pipe flows. Finite Elements in Water Resources. Proc. 4th Int. Conf. Hanover, Germany, 1982.

[3] Fox, J. A., Hydraulic Analysis of Unsteady Flow in Pipe Networks. MacMillan, London, 1977.

[4] Streeter, V. L., and E. B. Wylie, Hydraulic Transients. McGraw-Hill, New York, 1967.

[5] Harris, G. S., Real time routing of flood hydrographs in storm savers. J. Hyd. Div., A.S.C.E., 96, HY6, 1970.

[6] Wylie, E. B., Unsteady free surface flow computations. J. Hyd. Div., A.S.C.E., 96, HY11, 1970.

[7] Lister, M., The numerical solutions of hyperbolic partial differential equations by the method of characteristics. Mathematical Methods for Digital Computers, Ralston and Wilf, eds., John Wiley & Sons, 1960.

[8] Mozayeng, B., and C. S. Song, Propagation of flood waves in open channels. J. Hyd. Div., A.S.C.E., 95, HY3, 1969.

[9] Zovne, J. J., and C. S. Martin, Simulation of transient supercritical channel flow. J. Hyd. Div., A.S.C.E., 105, HY7, 1979.

[10] Jolly, J. P., and V. Yevjevich, Simulation accuracies of gradually varied flow. J. Hyd. Div., A.S.C.E., 100, HY7, 1974.

[11] Sivaloganathan, K., Comparative study of characteristic methods for free surface flow computations. Proc. Int. Conf. on Urban Storm Drainage, Southampton, 1978.

[12] Sivaloganathan, K., Channel flow computations using characteristics. J. Hyd. Div., A.S.C.E., 105, HY7, 1979.

[13] Hamming, R. W., Numerical Methods for Scientists and Engineers, McGraw-Hill, 1973.

[14] Spencer, A. J. M. et al. Engineering Mathematics. Van Nostrand Reinhold, England, 1977.

Technical News Briefs

New Technical Developments

SENSOR SYSTEM MONITORS SURFACE ROUGHNESS/TOOL CONDITION FOR AUTOMATED MANUFACTURING

An ultrasonic system has been developed to monitor the surface finish of stationary or moving surfaces. Pulsed ultrasound is guided from a source transducer to the monitored surface by a flowing stream of liquid. Part of the ultrasound interacts with the monitored surface and is back-scattered up the liquid stream to the same transducer. The amplitude of the returned ultrasound is related to the roughness of the surface.

The system was motivated by the need for in-process part monitoring during automated manufacturing. It was designed to take advantage of the cooling systems that are used commonly on high-speed metal-cutting machinery to flood the work piece with a cooling and lubricating fluid. The steady stream of coolant acts as a guide to "couple" the ultrasound to the surface of the part.

Surfaces with average roughness values from 25 to 1000 microinches have been studied. A resolution of about 25 microinches appears to be possible. Cylindrical surfaces rotating with surface speeds in excess of 1000 feet/min have also been successfully monitored.

In addition to monitoring part finish in real time and in situ the system provides the basis for a much improved tool-control strategy. Using sensory feedback, when the system detects an unacceptable surface finish due to worn or chipped tooling, a "change tool" order can be given to a machining or turning center.

Additional work is being performed at higher frequencies necessary for smoother surfaces and a prototype is being developed for testing on a machining center in the NBS Automated Manufacturing Research Facility. A patent on the system is being applied for.

For further information contact G. V. Blessing, National Bureau of Standards, Gaithersburg, MD 20899.

ULTRASONIC SENSOR DEVELOPED TO CHARACTERIZE SURFACE MODIFIED METALS

A new ultrasonic sensor system for measuring the depth and elastic properties of treated surfaces of steels and other metal alloys has been developed by an NBS scientist and two guest workers from Johns Hopkins University.

The sensor system is made up to two transducers, one to launch ultrasonic waves and another to receive them as they move across the surface of the materials [1]. By precise measurements of the velocity of the ultrasonic waves, the thickness and elastic properties of the modified surface are determined. The homogeneity of the surface layer can be examined, and flaws or any delaminations that may exist between the modified surface layer and the substrate can be detected.

One of the important advantages offered by the new ultrasonic sensor is that the waves can be sent over irregular or curved surfaces of metal components to accurately estimate the depths and properties of modified surface areas. It is the only known method for making the measurements without destroying the finished material.

Research on the ultrasonic sensor was performed as part of a program to develop nondestructive evaluation techniques for new rapid solidification technologies.

Additional developments using noncontact ultrasonic transduction techniques such as those based on lasers or electromagnetic acoustic transducers may lead to in-process sensor systems to measure metal product characteristics at various points in the manufacturing process.

References

[1] Elkind, B. J.; M. Rosen and H. N. G. Wadley, Ultrasonic characterization of surface modified layers, to appear in METRONS, Series A.

IMPROVED FLEXURE–HINGE INSTRUMENT STAGE PATENTED

A patent has been granted for an improved positioning stage for precision measurement instruments. The development is based on a new design for the so-called "flexure" hinge [1]. Flexure hinges are made by cutting out material from opposite sides of a normally rigid member, such as a steel bar, leaving only a thin web-like section at that point. Such hinges are sometimes used in precision machinery—in this case a positionable specimen stage for microtopographic mapping.

The NBS patent [2] covers a new design for the flexure hinge that allows the flexing member to elongate slightly while bending. The new hinge is incorporated in a stage that is capable of smooth motion in an almost perfect plane along either the x- or y-axis without sideways displacement. In the prototype version of the stage, pitch, roll, and yaw were no greater than 3 arc-seconds for both x and y motion, corresponding to deviations on the order of 10 nanometers. Within its limits of motion (a 5-mm square), it improves on stages with conventional flexure hinges, which cannot move along one axis without some movement along the other; and on stages that achieve straight-line movement using mechanical sliding joints or roller-element bearings, which cannot move as smoothly as a flexure stage.

References

[1] Teague, E. C.; R. D. Young, F. E. Scire, and D. Gilsinn, Para-flex stage for microtopographic mapping, to appear in Rev. Sci. Inst.

[2] Scire, F. E. and E. C. Teague, Flexure hinge, U.S. Patent No. 4,559,717; December 24, 1985.

HEAT PIPE OVEN AS A SOURCE FOR MOLECULAR BEAMS

A heat pipe oven source for a molecular beam has been developed [1] as a superior source for atoms or molecules to be used in atomic frequency standards. The oven can also be used in studies of atomic and molecular properties. The new oven is an improvement over earlier ovens in that it limits the amount of non-useful materials ejected from the oven, by being insensitive to orientation or acceleration and by eliminating the normally used small collimation channels that are easily plugged.

The oven consists of a hollow cylinder made of porous material, such as tungsten, molybdenum, stainless steel, or alumina silicates that can be wetted by the material used in the beam. One end of the cylinder is closed and the working material there is heated to evaporation forming a beam that is partially collimated, as determined by the diameter to length of the oven. Material that is not ejected in the beam strikes the wetted porous sides of the oven and is carried back to the hot end by wick action for re-use. This gives the device a longer operating life than conventional for a given amount of material.

For further information contact R. Drullinger, National Bureau of Standards, Boulder, CO 80303.

References

[1] Drullinger, R., Heat pipe oven, U.S. Patent No. 4, 558, 218.

NBS ESTABLISHES STANDARD FOR COMPUTER PASSWORD USAGE

Passwords have been used for centuries to prove authorization to access valuable items. Today, they commonly are used to help control access to computer systems, data files, and networks. It is recognized that passwords are neither the only nor necessarily the best method of controlling access. However, if properly used, they can provide a reasonable level of protection.

A difficulty for computer system managers and users was the lack of standard usage requirements. As a result, password-based access control mechanisms were often inconsistent and ineffective. There was no agreement on such issues as minimum password length, lifetime (time between changes), or composition. To address this need, NBS recently published Federal Information Processing Standard 112, *Password Usage* [1], which establishes minimum password usage requirements for those computer systems using passwords although it does not require that passwords be used in all systems).

Federal Information Standards Publications (FIPS PUBS) are the vehicles by which a wide range of information processing standards and publications are issued to Federal Government computer users. These standards are mandatory for Federal agencies, and they are often adopted by private sector organizations. Of the more than 100 FIPS pubs issued over the years, several have addressed the issues of computer security.

Two types of password are defined: *personal passwords* which are used to authenticate a claimed identity (Example: "I am Joe Smith. I prove this by giving you my password. 'CLAPFOBS'."), and *access passwords* which are used to validate claims of access for systems resources such as data files (Example: The password for file PAYROLL is 'HOKFUST'.)

The Password Usage Standard lists 10 factors affecting password usage and minimum criteria for each area. The factors are:

Composition	–Types of characters that can be used in a password.
Length	–Minimum and maximum number of characters in a password.
Lifetime	–Maximum time a password is valid.
Source	–Who generates the passwords?
Ownership	–Who controls the passwords?
Distribution	–How are new passwords communicated to the user?
Storage	–How are passwords stored and protected?
Entry	–How are passwords entered into the system by a user?
Transmission	–How are passwords protected between entry by the user and receipt by the system?
Authentication Period	–For how long is the authentication established by a password valid?

Criteria are established both for manually administrated password systems and for automated password administration mechanisms.

It is important to note that this standard is applicable for a broad range of uses, from large-scale, multi-user computer systems to personal computer systems, wherever passwords are used.

This new standard will help computer system managers and security officers measure their level of compliance with minimum password management requirements—something they were unable to do before. Since password-based access controls are used as the primary access control mechanism in almost all computer systems, this standard will provide significant improvement in the overall security and protection afforded valuable data and information resources throughout the Federal Government.

References

[1] FIPS PUB 112, *Password Usage*, National Technical Information Service (NTIS), Springfield, VA 22161; $9.95.

INTER-ELEMENT INTERACTIONS IN LARGE PHASED ARRAY ANTENNAS

It is difficult to obtain information on the electromagnetic fields produced by large phased array antennas at large distances (far filed patterns). However, the field patterns of the sub-arrays which form the building blocks of such arrays are well known and can be accurately measured. A procedure is being developed [1] to predict the far field patterns of phased array systems from the elementary patterns formed by the sub-arrays. The analysis to date has been limited to one-dimensional arrays and does not include the effects of multiple reflections on the sub-array field patterns, but future work is planned to extend the formalism already developed. A major goal of this work is to be able to predict the far field patterns of a large phased array using input data obtained from measurements in the near field from the sub-arrays.

References

[1] Muth, L. A., Interelement interactions in phased arrays: Theory, methods of data analysis, and theoretical simulations, NBS Technical Note 1091 (1985).

A MEASUREMENT SYSTEM FOR DETERMINING THE POWER DELIVERED TO AN ANTENNA

Standard gain horn antennas are used in the National Bureau of Standards anechoic chamber to produce well-characterized electromagnetic fields. A major uncertainty in the calibration procedure arises from the uncertainty in the net power delivered to the antenna. A procedure has been developed for measuring the net power delivered and evaluating its uncertainty [1]. This procedure permits the automated system used to establish known electromagnetic fields to be largely self-calibrating; this is possible since the key parameters upon which the net power delivered to the antenna depend can be obtained directly by replacing either the antenna or one of the power meters in the system by loads with known characteristics.

References

[1] Kanda, M. and R. D. Orr, A radio-frequency power delivery system: Procedures for error analysis and self-calibration. NBS Technical Note 1083 (1985).

New Standard Reference Materials*

STANDARD ACID SOLUTIONS FOR DETERMINATION OF pH IN RAINWATER

In November, 1983, 12 laboratories agreed to participate in an interlaboratory test of pH measurements in rainwater [1]. The tests were conducted to determine the feasibility of using dilute solutions of

*SRMs can be ordered from the Office of Standard Reference Material, NBS, Gaithersburg, MD 20899, Telephone 301-921-2045.

a strong acid as working standrds for pH measurements in acid deposition studies. Scientists at the National Bureau of Standards independently tested sets of the acid samples.

Results of ruggedness test experiments, which were also conducted, showed that stirring has an adverse effect on the measurement of pH of dilute acid solutions by amplifyng the random noise and biasing the measured values. Moderate temperature control (±0.5 degree C) was found to be sufficient for maintaining measurements accurate to 0.01 pH unit. The results also demonstrated that the addition of neutral salts cannot be tolerated in accurate pH measurements because these salts change the mean activity coefficients of solutions, and also unpredictably change the electrode behavior and hence, the measured pH.

The use of standard acid solutions is recommended for all those involved in network monitoring of wet deposition to improve the intercomparability of the measurements as a function of time and location. To aid in this endeavor, Standard Reference Material, SRM 2694, Simulated Rainwater, has been prepared and analyzed and is available through the Office of Standard Reference Materials. The SRM consists of a set of two 50 mL solutions in polyethylene bottles. The nominal pH of Level I is 4.3 and that of Level II is 3.6. The acidity and the specific conductance have also been determined, as well as several of the major cations and anions commonly found in rainwater.

References

[1] J. Res. Natl. Bur. Stand. 91-1 (1986).

NEW MATERIAL TO IMPROVE MEASUREMENTS OF PCB LEVELS IN BLOOD

Tests for amounts of polychlorinated biphenyls (PCBs) in blood samples can be checked for accuracy with a standard reference material (SRM) now available from the National Bureau of Standards. Such tests are important for determining the exposure to the toxic compounds of chemical industry employees or others who must work with PCBs.

SRM 1589 consists of freeze-dried human blood serum which is "spiked" with 106 nanograms of Aroclor 1260 per gram of serum. Aroclor 1260 is a mixture of PCBs found in some transformer oils. The SRM, which must be reconstituted with 10 milliliters of distilled water, is intended for use in the calibration of analytical instruments used for measuring the concentration of PCBs in blood. It also may be used as a primary standard against which secondary reference materials may be compared. Certified to be accurate within 1 percent range, the SRM costs $163 for a three-vial set.

ENVIRONMENTAL STANDARD DEVELOPED FOR USED LUBRICATING OIL

Regulations of the Environmental Protection Agency require that used oils which contain more than 50 parts per million of chlorine must be analyzed for the presence of polychlorinated biphenyls (PCBs), which are toxic compounds. Samples which do, or do not, have to undergo analysis for PCB content can be identified by tests which show the total concentration of chlorine in a used lubricating base oil. A new standard reference material, SRM 1818 (Total Chlorine in Lubricating Base Oil), consists of a series of five 20-gram ampules of re-refined lubricating base oils having total chlorine concentrations ranging from 30 to 600 parts per million. The cost is $200.

NEW GLASS STANDARDS CERTIFIED FOR CHEMICAL CONTENT

The chemical composition of glass is important in determining its properties, such as thermal performance, resistance to radiation, electrical conductivity and durability. In order to aid glass manufacturers and the designers of glass products who require specific material performance, the ASTM Committee C14 Committee on glass and glass products has recently revised recommended procedures for the determination of the chemical composition of glass. The improved procedures include conventional techniques such as wet chemical analysis, as well as x-ray fluorescence and neutron activation analysis.

Use of the new procedures for the chemical analysis of glass will be facilitated by three new standard reference materials. SRM 1411 (Soft Borosilicate Glass), SRM 1412 (Multicomponent Glass), and SRM 1413 (High Alumina Sand). These SRMs are expected to play a key role in quality control and product performance, the research and development of new glasses, and in the manufacture of better quality glasses. The cost of the new SRMs is $172 per unit.

Journal of Research of the National Bureau of Standards

Conference Reports

ELECTROPHORESIS SOCIETY MEETING HOSTED AT NBS

by Dennis J. Reeder, Diane K. Hancock, Jesse J. Edwards, and Kristy L. Richie

Center for Analytical Chemistry
National Measurement Laboratory
National Bureau of Standards

The National Bureau of Standards (NBS) hosted the Electrophoresis Society Meeting March 26–28, 1986. The meeting, co-sponsored by the Society and the Center for Analytical Chemistry, drew about 135 scientists. The participants represented industry (40 percent); local, State, and Federal government agencies (40 percent); and universities or university hospitals (20 percent).

The meeting was structured to allow maximum interaction among the participants. Morning plenary sessions were held in the Green Auditorium and afternoon sessions in the Gaithersburg Holiday Inn. Ten companies demonstrated their latest instrumentation in a commercial exhibit.

In the first plenary session, Bruce Budowle of the Forensic Science Research and Training Center, Federal Bureau of Investigation, showed advances in the technology of making ultrathin-layer polyacrylamide gel isoelectric focusing a more reproducible method. The method is becoming a useful tool in forensic analyses and has shown remarkable versatility in its adaptation for genetic analyses of small amounts of human body fluids.

John Fawcett presented a comprehensive and detailed review of comparisons between ordinary isoelectric focusing and electrofocusing in immobilized pH gradients. His work with Andreas Chrambach of the National Institutes of Health (NIH) provided insight into such criteria as resolving power, reproducibility, susceptibility to pH and voltage measurement, ease of protein isolation, preparative load capacity and purity of product.

Carl Merril (NIH) provided a historical background to the process of silver staining of proteins. He gave examples of how detection techniques have progressed from direct observation of protein-coated microspheres and colored proteins, requiring milligram amounts, to the detection of proteins by their ultraviolet absorption, to labelling with radionuclides, to direct staining with organic fluorescent dyes, and most recently to silver stains which require only a tenth of a nanogram. He also demonstrated how most protein stains and autoradiographic methods exhibit protein-specific quantitative optical density/concentration relationships, which are indicative of the dependence of detection methods on the content of specific groups within each protein.

Norman Anderson of Proteus Technologies, Inc., spoke on the subject of future directions of electrophoresis, with particular emphasis on the role that electrophoresis will play in biotechnology application areas that include exploring the human genome and newer areas relating to improvements in plant breeding and production of better plant products.

Philip Serwer from the University of Texas Health Science Center, San Antonio, detailed the separation of viruses and viral components in extracts of infected cells by use of agarose gel electrophoresis. This technique is comparatively inexpensive and nonselective for the detection of particles in either unfractionated or partially-

fractionated lysates of infected cells. Spheres can be discriminated from rods by measurement of electrophoretic mobility as a function of gel concentration. Dr. Serwer also showed the use of agarose in two-dimensional applications.

Nancy Stellwagen, University of Iowa, concluded the plenary sessions by summarizing the current interest in gel electrophoresis of DNA molecules. Of particular interest was her description of the use of pulsed electric fields for the separation of chromosome-sized molecules of DNA. Using alternating inhomogeneous electric fields for separation and the application of electric birefringence to study the orientation of DNA molecules, Dr. Stellwagen researched several theories on the process of DNA separation. In particular, the reptation theory for electrophoresis based in the axial movement ("snaking") of DNA molecules through gels seems to have validity and can be expressed in appropriate mathematical equations.

. . . pulsed electric fields for the separation of chromosome-sized molecules of DNA . . .

Although not a formal presentation, the review paper by Susan Olson and Carl Merril was included in the Proceedings publication because of its timely and detailed information regarding the separation of peptides on different media. The extensive bibliography should be useful to anyone beginning work with this technology.

The extensive bibliography should be useful to anyone beginning work with this technology.

The afternoon meetings were held in an informal setting in order to give the participants ample opportunity to interact and discuss their findings. The clinical session was combined with the genetics session to yield a lively and interesting session dealing with diagnostic capabilities of electrophoresis. Of note was the series of talks given by the University of Michigan researchers led by Samir Hanash. Dr. Hanash made extensive use of two-dimensional polyacrylamide gel electrophoresis in the study of acute lymphoblastic leukemia. One particular polypeptide designated L3 with a molecular weight of 29,000 showed substantial variability in the staining intensity depending upon the patient being tested. If the spot was intense, very few of the patients relapsed, if the spot was weak, there was a strong likelihood of an unfavorable outcome in the disease process. Thus, detailed analysis of the polypeptide constituents of leukemic cells, made possible by two-dimensional electrophoresis, has the potential of aiding physicians in the treatment of lymphoblastic leukemia.

In the gel media session, participants presented results of their work with newer types of gel media. In particular, a recently introduced derivatized agarose called "Nufix Glyoxyl Agarose" (FMC-Marine Colloids) was discussed. The wide spectrum of glyoxyl agarose properties were presented, including its controllable reactivity toward primary and secondary amines, its native fixation capabilities, and its ability to be cast in any form. A glyoxyl agarose/polyacrylamide gel composite permits in situ immobilization of polypeptides after electrophoretic separation. The application of glyoxyl agarose to blotting and chromatography was also discussed. Also reported was the effect of borate buffers on increased sieving properties of agarose gels. This sieving increase is most pronounced if the borate is present during casting of the gel. Borate also alters agarose viscosity and gel strength, as well as gelling and melting temperatures. Recently reported research on the properties of rehydratable gels has now come to a point of potential standardization. A report was presented by Kristy Richie of NBS on a interlaboratory comparison study of rehydratable gel reproducibility with standard protein preparations. In comparing laboratory results, she noted that there were distinguishable variations in the protein band patterns of the same protein due to several factors in the electrophoretic run. Factors such as electrode separation distance, composition of catholyte and anolyte, temperature, humidity, and time of the electrophoretic run, all influenced the electrophoretic patterns. The second round robin analysis will include more instructions and details for controlling the influencing factors.

. . . electrode separation distance, composition of catholyte and anolyte, temperature, humidity, and time of the electrophoretic run, all influence the electrophoretic patterns.

Philippe Arnaud (NIH) compared commonly used nitrocellulose membrane transfer material with the newer zeta probe membranes made of Nylon. His data demonstrated the possibility of "leakage" of a protein of interest from nitrocellulose, but transferred with much tighter binding to the zeta probe membrane. In particular, although different

higher weight molecular forms of alpha$_1$-acid glycoprotein (A_1S) transfer and bind with nitrocellulose, the monomer did not appear to transfer. However, when the zeta probe material was used, the monomer was clearly transferred from the polyacrylamide gel slab and represented the major molecular species of A_1S.

The round table discussion on immobilized pH gradients (IPG) centered on sharing ingenious methods for circumventing various problems encountered with the technique. One such problem is that of solubilizing proteins so that they could enter into the gel matrix. Some laboratories found that addition of 2 mol/L urea to the sample or to the equilibration solution was a useful procedure, while other researchers added carboydrate such as dextrans or agarose to the gel. Some proteins can be applied to the gel surface while others need to be applied to the holes cut into the gel. Examples of analytical and preparative one-dimensional applications were presented as well as two-dimensional applications. Angelika Görg (Technische Universität München) showed excellent resolution of human plasma proteins in a two-dimensional system that utilized immobilized pH gradients as the first dimension. There is continuing evidence that many of the early problems and pitfalls encountered when using immobilized pH gradient technology are now being solved. Examples of very high resolution capabilities were demonstrated.

. . . ingenious methods for circumventing various problems . . .

In the session on two-dimensional electrophoresis, the leading topic discussion centered around the requirements for data reduction of protein patterns generated by two-dimensional electrophoresis. Guidelines presented for the development of a model protein database were followed by an assessment of the functions and effective uses of such a system as a medium for communicating information. These presentations stimulated much discussion about the types of experiments that are necessary to produce the maximum amount of useful data. Problems associated with data reduction of protein patterns became apparent when approaches to the methods of spot detection and quantification (e.g., parametric versus non-parametric analysis) were presented. This led to extensive discussion of the theoretical and practical aspects of image analysis. Problems of standardization in both isoelectric focusing and SDS-electrophoresis were addressed with emphasis upon the need for commercially-available products of high purity and good reproducibility. The reliability of marker proteins, the acceptable limitations for purity and reproducibility and the problems of production and storage were discussed. It was encouraging to hear of the high priority that commercial firms are placing on standardization of products and techniques. The results of these efforts were shown in the presentation of cleaner molecular weight markers and high quality carbamylated charge trains for isoelectric focusing. Finally, procedures for sample preparation and evaluation were discussed. Data were presented which evaluated sample preparation by ultrafiltration and diafiltration using centrifugal microconcentrators. Also, a novel total protein assay using UV-difference spectroscopy was presented. Results compared favorably with other protein assay methods such as Coomassie dye binding, bicinchoninic acid and the so-called "Lowry" method.

Problems associated with data reduction of protein patterns became apparent . . .

Current interest in protein detection techniques were aptly displayed by the attendees of the staining session. Joseph Yudelson (Kodak), developer of the nickel protein stain, presented information on the chemistry, nucleation, and amplification process in the nickel and silver visualization systems. These systems which are akin to physical development in the photographic field require formation of critical nucleation clusters if grain formation is to occur. In the case of the nickel stain, palladium serves as the nucleation agent, causing the protein to become a catalytic development center. In the case of silver stain, a much larger number of species (metals, metal oxides, and sulfides) serve as nucleation agents. The stronger the reducing agent in the developer, the smaller the critical cluster size required for the metal reduction to proceed autocatalytically. Hence the alkaline formaldehyde reducer used in the silver stain requires only approximately two silver atoms for critical cluster size while the dimethylamine borane used in the nickel stain requires a larger critical cluster size. These differences account for the greater instability of the silver physical developer but also for its somewhat greater sensitivity. Dr.

. . . akin to physical development in the photographic field . . .

Yudelson presented calculations indicating that the silver stain is presently near its limit of sensitivity.

Diane Hancock (NBS) spoke on efforts to probe the mechanism of the silver stain with the goal of establishing staining conditions to increase sensitivity, and to decrease background staining. Data from various preliminary silver-protein binding studies were presented and discussed. Binding ratios on the order of 25 to 1 were found for the titrations of bovine serum albumin with $AgNO_3$ (silver nitrate) where silver concentrations were monitored with a silver ion specific electrode. Neutron activation analysis was used to determine silver distribution in polyacrylamide slab gels stained with either a Merril-type silver stain or with an ammonical silver stain. Highest silver concentrations were found in the stained protein bands, though substantial silver was present throughout the gel and the lowest concentrations were found in areas of negative staining. Results of feasibility studies using ^{109}Ag Nuclear Magnetic Resonance spectrometry (NMR) to identify silver-protein binding sites were presented. The data indicated that solution dynamics were such that little useful information could be obtained with this technique.

Betty Mansfield (Oak Ridge National Laboratory) presented a fluorescence assay method for determining 2,5-diphenyloxazole (PPO) concentrations from scintillation fluids. This analysis results in a considerable savings of time as the solution can now be regenerated many times before the expensive PPO must be precipitated, filtered, and dried.

The final sessions devoted to nucleic acids and particle electrophoresis brought together experts who focused their attention on physical characterization of materials separated in agarose gel electrophoresis. Considerable attentioan was given to a system developed by Douglas Gersten, Georgetown University, for automated nucleic acid electrophoresis and hybridization analysis.

. . . sessions devoted to nucleic acids and particle electrophoresis brought together experts who focused their attention on physical characterization of materials . . .

The Electrophoresis Society Workshop was successful in bringing together authorities who could demonstrate the latest techniques in electrophoresis. Participants observed ultrathin methods for forensic analyses presented by Bruce Budowle and Dale Dykes. Robert Allen and Calvin Saravis showed how electrophoresis and enzyme staining could be performed very rapidly on the same apparatus. Comparisons of equipment capabilities using the same samples were demonstrated by Hoefer Scientific Instruments and Haake Buchler Instruments. The new "Phast" system for high-performance electrophoresis was demonstrated by Pharmacia, Inc.

Commercial workshops held during the first two days of the meeting were also well attended. Hoefer Scientific Instruments presented a workshop on minigel electrophoresis and Western blotting. Protein Databases demonstrated the use of a new system, "PDQuest" for 2-D Gel Analysis. Pharmacia, Inc., introduced the "Phast System" for high-performance electrophoresis to the participants. This highly automated system had only been introduced to the scientific community at a meeting in Washington, DC, two days before the Society meeting. LKB, Inc., presented topics on electrofocusing and immobilized pH gradients. Angelika Görg, a renowned expert in the field, provided interesting insights into the separations process.

In summary, the meeting provided excellent opportunities to learn of the newest techniques and equipment in electrophoresis. It probed the diversity of directions that the field of electrophoresis is taking, hosting numerous stimulating discussions and problem solving sessions along the way. As a beneficial result of the meeting, approaches to problems developed as industrial manufacturers were exposed to the challenges encountered by the researchers using electrophoresis.

. . . the meeting . . . probed the diversity of directions . . .